Defence Research and Development Canada
Recherche et développement pour la défense Canada

DEFENCE DÉFENSE

Array of Laminated Waveguides for Implementation in LTCC Technology

Michel Clénet, Yahia M. M. Antar and David Lee

Defence R&D Canada – Ottawa
TECHNICAL MEMORANDUM
DRDC Ottawa TM 2006-227
November 2006

Canada

Report Documentation Page					*Form Approved* *OMB No. 0704-0188*

Public reporting burden for the collection of information is estimated to average 1 hour per response, including the time for reviewing instructions, searching existing data sources, gathering and maintaining the data needed, and completing and reviewing the collection of information. Send comments regarding this burden estimate or any other aspect of this collection of information, including suggestions for reducing this burden, to Washington Headquarters Services, Directorate for Information Operations and Reports, 1215 Jefferson Davis Highway, Suite 1204, Arlington VA 22202-4302. Respondents should be aware that notwithstanding any other provision of law, no person shall be subject to a penalty for failing to comply with a collection of information if it does not display a currently valid OMB control number.

1. REPORT DATE **NOV 2006**	2. REPORT TYPE **N/A**	3. DATES COVERED **-**
4. TITLE AND SUBTITLE **Array of Laminated Waveguides for Implementation in LTCC Technology**		5a. CONTRACT NUMBER
		5b. GRANT NUMBER
		5c. PROGRAM ELEMENT NUMBER
6. AUTHOR(S)		5d. PROJECT NUMBER
		5e. TASK NUMBER
		5f. WORK UNIT NUMBER
7. PERFORMING ORGANIZATION NAME(S) AND ADDRESS(ES) **Defence R&D Canada - Ottawa Technical Memorandum DRDC Ottawa TM 2006-227 Canada**		8. PERFORMING ORGANIZATION REPORT NUMBER
9. SPONSORING/MONITORING AGENCY NAME(S) AND ADDRESS(ES)		10. SPONSOR/MONITOR'S ACRONYM(S)
		11. SPONSOR/MONITOR'S REPORT NUMBER(S)
12. DISTRIBUTION/AVAILABILITY STATEMENT **Approved for public release, distribution unlimited**		
13. SUPPLEMENTARY NOTES **The original document contains color images.**		
14. ABSTRACT		
15. SUBJECT TERMS		

16. SECURITY CLASSIFICATION OF:			17. LIMITATION OF ABSTRACT	18. NUMBER OF PAGES	19a. NAME OF RESPONSIBLE PERSON
a. REPORT **unclassified**	b. ABSTRACT **unclassified**	c. THIS PAGE **unclassified**	**SAR**	**80**	

Array of Laminated Waveguides for Implementation in LTCC Technology

Michel Clénet
DRDC Ottawa

Yahia M. M. Antar
Royal Military College of Canada

David Lee
Communications Research Centre

Defence R&D Canada – Ottawa

Technical Memorandum

DRDC Ottawa TM 2006-227

November 2006

Author

Original signed by Michel Clénet

Michel Clénet

Approved by

Original signed by Darren Baker

Darren Baker

Head / CNEW Section

Approved for release by

Original signed by Cam Boulet

Cam Boulet

Head / Document Review Panel

Abstract

This document reports on the study of a five-element array prototype developed for communications in K-band and suitable for LTCC technology. The radiating element is an open waveguide realised in laminated technology. A novel coaxial-to-waveguide transition has also been designed as feed port for measuring the prototypes. The design, analysis, fabrication process and measurement of this antenna element were described in a previous report. To summarize, the element exhibits a 1 GHz bandwidth around a 20.7 GHz centre frequency. The element radiation pattern indicates a gain of 2.7 dBi. This new antenna is suitable for brick architecture array configuration. In an array configuration the input impedance of each radiating element is slightly perturbed by the proximity of the other antennas. The mutual coupling between the elements, however, remains below –20 dB across the bandwidth. The simulated boresight radiation pattern of a five-element array is stable over the bandwidth and the gain reaches 9.2 dBi at 20.7 GHz. These results are confirmed by the measurement. The scanned radiation patterns obtained by simulation show a good behaviour of this array for scan angles up to 50^{o}. The measured radiation patterns for several scan angles demonstrate the scanning capability of this array.

Résumé

Ce document décrit l'étude d'un réseau de cinq antennes développé pour des systèmes de communications en bande K, et de technologie compatible avec la technologie LTCC. L'élément rayonnant est un guide d'onde ouvert réalisé avec un matériau laminé. Une nouvelle transition coaxial-guide d'onde a également été développée pour connecter l'élément rayonnant aux systèmes de mesure. La conception, l'analyse, le procédé de fabrication et les mesures ont été reportés dans un précédent document. En résumé, l'élément rayonnant a une bande passante de 1 GHz centrée autour de 20.7 GHz. Les diagrammes de rayonnement indiquent un gain de 2.7 dBi à 20.7 GHz. Cette nouvelle antenne peut être utilisée dans des réseaux d'architecture de type « brique ». En configuration réseau, l'impédance d'entrée de chaque élément rayonnant est légèrement perturbée par la proximité des autres antennes. Le couplage entre éléments est néanmoins inferieur à -20 dB sur toute la bande passante. Les diagrammes de rayonnement obtenus par simulation sont stables sur toute la bande passante, et le gain atteint 9.2 dBi à 20.7 GHz. Ces résultats sont confirmés par la mesure. Les diagrammes de rayonnement de balayage obtenus par simulation montrent que ce réseau peut être utilisé comme réseau à déphasage pour des angles de balayage allant jusqu'à 50^{o}. Les diagrammes mesurés pour plusieurs angles de balayage ont confirmé les capacités de balayage de ce réseau.

This page intentionally left blank.

Executive summary

This document reports on the study of a five-element array prototype developed for communications in K-band and suitable for LTCC technology. The radiating element is an open waveguide realised in laminated technology. In this design the vertical walls are created with vias. A novel coaxial-to-waveguide transition has also been designed as feed port for measuring the prototypes. The design, analysis, fabrication process and measurement of this antenna element were described in detail in a previous report. But for a better understanding a summary of the design procedure and the main results for this radiating element are provided. To summarize, the impedance bandwidth of the coaxial-to-waveguide transition is very wide (17 GHz to more than 25 GHz), but the aperture matching circuit narrows down the impedance bandwidth of the radiating element to 1 GHz around a 20.7 GHz centre frequency. The element radiation pattern indicates a gain of 2.7 dBi, half-power beamwidths of 122^o and 64^o in the E- and H-planes, respectively, and a cross-polarization level lower than -20 dB.

Based on the good agreement obtained between simulation and measurement for a single element, a five-element array was designed, fabricated and analysed. This array is suitable for brick architecture array configurations. In array configuration the element impedance bandwidth is slightly shifted up in frequency due to the mutual coupling, which however remains below –20 dB in the worst case. The radiation patterns of the array are stable across the operating bandwidth (20.2 GHz to 21.2 GHz) and the measured gain is 9.2 dBi at the centre frequency. The array exhibits a half-power beamwidth of the order of 22^o in the plane of the array, and a cross-polarization level lower than -20 dB. The measurements were confirmed by the results obtained by simulation. This array also shows a good scanning behaviour up to 50^o. Measurements of radiation patterns for several scan angles have demonstrated the scanning capability of this array.

The results obtained with our prototypes point out some issues regarding the effects of fabrication tolerances. These issues will be considerably reduced if the elements are realised with LTCC process. In fact, to our knowledge, fabrication tolerances are more controlled with the LTCC process than with our PCB fabrication process.

Laminated waveguides are suitable for applications when the total substrate thickness is important compared to the wavelength. This design can be scaled for higher frequency applications, or when a material of higher permittivity is used. The work reported here concentrates on a radiating element in laminated technology to be used in array configuration for scanning applications. For this reason, an open waveguide was chosen rather than a horn to obtain a large beamwidth, and therefore a low gain. A study focusing on high-gain element using laminated technology will be complementary to this first investigation on radiating laminated waveguides.

Clénet, M, Antar, Y. M. M., Lee, D., 2006. Array of Laminated Waveguides for Implementation in LTCC technology. DRDC Ottawa TM 2006-227, Defence R&D Canada – Ottawa.

This page intentionally left blank.

Sommaire

Ce document décrit l’étude d’un réseau de cinq antennes développé pour des systèmes de communications en bande K, et de technologie compatible avec la technologie LTCC. L’élément rayonnant est un guide d’onde ouvert réalisé avec un matériau laminé. Dans cette technologie les parois verticales sont réalisées avec des trous métallisés. Une nouvelle transition coaxial-guide d’onde a également été développée pour connecter l’élément rayonnant aux systèmes de mesure. La conception, l’analyse, le procédé de fabrication et les mesures ont été reportés en détail dans un précédent document. Pour une meilleure compréhension ce rapport décrit succinctement la procédure de conception et les principaux résultats. En résumé, la bande passante de l’élément rayonnant est très large (de 17 GHz à plus de 25 GHz), mais le circuit d’adaptation à l’ouverture du guide la réduit à une bande passante de 1 GHz centrée autour de 20.7 GHz. Les diagrammes de rayonnement indiquent un gain de 2.7 dBi à 20.7 GHz, des ouvertures à mi-puissance dans les plans E et H de 122^o et 64^o respectivement, et un niveau de polarisation croisée inférieur à -20 dB.

D’après la bonne concordance entre les résultats issus des simulations et des mesures de cet élément rayonnant, un réseau de cinq antennes a été conçu, fabriqué et analysé. Ce réseau est compatible avec des réseaux d’architecture de type « brique ». En configuration réseau, l’impédance d’entrée de chaque élément rayonnant est légèrement perturbée par la proximité des autres antennes. Le couplage entre éléments est néanmoins inferieur à -20 dB sur toute la bande passante. Les diagrammes de rayonnement obtenus par simulation sont stables sur toute la bande passante (20.2-21.2 GHz). Ces résultats sont confirmés par la mesure. Le gain mesuré atteint 9.2 dBi à 20.7 GHz. L’ouverture à mi-puissance dans le plan contenant le réseau est d’environ 22^o et le niveau de polarisation croisée est inférieur à -20 dB. Les diagrammes de rayonnement de balayage obtenus par simulation montrent que ce réseau peut être utilisé comme réseau à déphasage pour des angles de balayage allant jusqu’à 50^o. Les diagrammes mesurés pour plusieurs angles de balayage ont confirmé les capacités de balayage de ce réseau.

Les résultats obtenus avec nos prototypes ont souligné quelques inquiétudes quant à l’effet des tolérances de fabrication. Ces effets seraient néanmoins considérablement réduits si les éléments étaient fabriqués avec la technologie LTCC. En fait, d’après nos connaissances actuelles, les tolérances de fabrications sont plus contrôlées avec le procédé de fabrication LTCC qu’avec le procédé de fabrication de circuits imprimés utilisé pour ce projet.

Les guides d’ondes réalisés avec des matériaux laminés, ou guides d’onde laminés, peuvent être utilisés pour des applications où l’épaisseur du matériau est importante par rapport à la longueur d’onde. Cette géométrie peut être réduite pour des applications haute-fréquence, ou pour des applications utilisant des matériaux à permittivité élevée. L’étude reportée dans ce document porte spécifiquement sur un élément rayonnant utilisé dans un réseau à déphasage. Pour cette raison, un guide d’onde ouvert fut choisi au lieu d’un cornet rayonnant, afin d’obtenir une ouverture à

mi-puissance large et donc un gain faible. Une étude centrée sur un élément à gain élevé réalisé avec un matériau laminée serait complémentaire à cette première étude sur les guides d'onde laminés.

Clénet, M, Antar, Y. M. M., Lee, D. 2006. Array of Laminated Waveguides for Implementation in LTCC technology. DRDC Ottawa TM 2006-227, R & D pour la défense Canada – Ottawa.

Table of contents

List of figures

List of tables

1. Introduction

This document reports on the study of a five-element array prototype developed for communications in K-band and suitable for LTCC technology. The radiating element is an open waveguides realised in laminated technology. A novel coaxial-to-waveguide transition has also been designed as feed port for measuring the prototypes. The design, analysis, fabrication process and measurement of this antenna element were described in a previous report [1]. But for a better understanding a summary of the design procedure and the main results for this radiating element are provided in this section. The study of a five element array was initiated in [1], but for some reasons the results obtained by simulation and measurement were not successful. This document presents a further study of the array of laminated waveguides, which has been more carefully carried out.

The design of the array and the simulation results are provided in section 2. Particular attention is given to the scan radiation characteristics. Section 3 continues with the measurement of the fabricated prototypes. The S-parameters, boresight and scan radiation patterns are reported and analysed. A conclusion summarizes the results and provides directions for future work.

1.1 Background

The idea of forming an integrated waveguide within an MIC (Microwave Integrated Circuit) substrate was postulated in [2] and [3]. The laminated waveguide (LWG) vertical walls are formed by a series of vias connecting the upper and lower ground planes. This guided structure has been mainly investigated as a low-loss microwave transmission line and to form various waveguide elements [2]-[5], and as a radiating element until recently [1],[6]. In a rectangular waveguide (RWG) propagating the dominant TE10 mode, there is only a vertical component of the electric field. Utilising the coordinates as defined in *Figure 1a*, the E-field would only have a component in the Y-direction. This means that to guide the travelling wave in the Z-direction, the walls must be able to provide a current flow along the vertical (Y) axis to reflect this electric field. This path for the current flow is provided by the vias of the LWG shown in Figure 1*b*. However, the spacing between vias, known as the pitch, must be kept sufficiently small such that the guided wave does not leak between the vias [3].

It has been demonstrated that the amount of leakage between the vias increases with the via pitch [3], [4]. The leakage, and subsequent losses, increases suddenly when the pitch exceeds $\lambda/4$ [2]. This forms the fundamental limit for the via pitch when designing laminated waveguides. Both the RWG and LWG can be designed to have lower losses than a planar transmission line in the SHF band (30GHz) [4]. However, the determination of the minimum via pitch is entirely dependent on the capability of the fabrication process.

The fabrication process targeted for this study is the low temperature co-fired ceramic (LTCC) technology. LTCC is a packaging technology that allows for electronic circuitry to be greatly reduced in size [7]-[9]. This is accomplished by stacking components on various levels and by using a moderate dielectric permittivity to reduce the electrical size of the components. Components, such as resistors and capacitors, can be directly integrated within the substrate thus eliminating the requirement for solder joints or wire bonds. Furthermore, as the ceramic substrate is a relatively good insulator, both digital and microwave circuitry can be alternately stacked and integrated within the same package [8]. Several antennas have been developed with LTCC technology [10]-[12], but none of them are endfire-type antennas.

Having the radiating element included in the package design reduces the interconnect complexity of RF front-end systems and therefore the production cost of the circuits. Compared to printed transmission lines embedded in a dielectric medium, waveguides have the particularity to confine the electromagnetic field into a closed area, thus avoiding coupling between transmission lines in a multilayer packaged system, or between buried radiating elements themselves in an array configuration [13]. In addition, the propagation attenuation in laminated waveguide technology is comparable to those of microstrip and stripline technologies [6].

a)

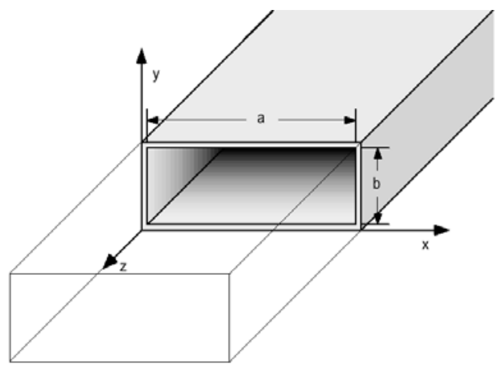

b)

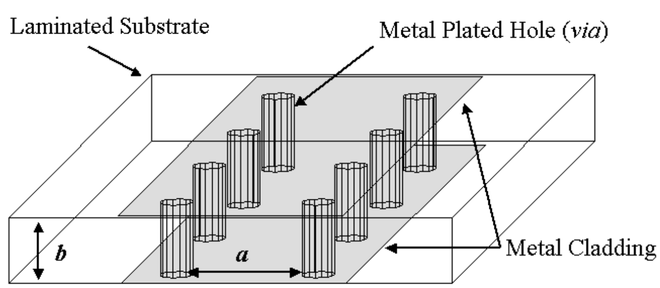

Figure 1. a) Rectangular waveguide and b) Laminated waveguide (drawing from[15] and [1])

The implementation of circuits in LTCC requires access to a foundry and can be cost prohibitive for prototyping limited runs. For this initial study, the laminated packaging process of LTCC is replicated by printed circuit board (PCB) fabrication techniques that allow for the stacking and bonding of various layers of dielectric material. The LTCC foundry design guidelines are followed to allow the design to be converted for future fabrication using the LTCC process. The Arlon CLTE substrate material is then chosen for fabrication.

The design of the radiating laminated waveguide is described in Section 2. The starting point is to consider the basic theory for rectangular waveguide to initiate the design. An electromagnetic model using Ansoft HFSS [14] is then presented. Particular attention is given to the description of a novel coaxial-to-waveguide transition, which is used to feed the waveguide through a K-connector. An aperture matching circuit to maximize the radiating power is also described. The results from simulation in terms of radiation characteristics are compared to the analytical solutions. Section 2 continues with the description of the fabricated prototypes and their measured characteristics. Based on the good simulation and measurement results for the element, a five-element array was designed and is presented in Section 3. The whole five-element array, which replicates as close as possible the fabricated prototype, has been simulated. Results from simulation in terms of S-parameters and radiation patterns are provided and analysed. The measurements of the five-element array prototype are finally presented and compared to the simulated results.

1.2 Simulation and measurement results for the laminated waveguide elements

The centre frequency for our application is 20.7 GHz. The dimensions of the waveguide are deduced using the frequencies of 17 and 25 GHz as cut-off frequencies for the TE10 and TE01 modes, respectively [1]. As the CLTE material (chosen for this application) is available at certain thicknesses only, the height of the waveguide is adjusted to a combination of dielectric material and bonding film. A final thickness of 3.49 mm is obtained using a 3.175 mm and 0.254 mm thick substrate layers bounded together with a 0.061 mm thick film. The corresponding TE01 cut-off frequency is 25.07 GHz. The width of the waveguide is 5.14 mm.

At the centre frequency of 20.7 GHz, a via pitch of 0.846 mm is found to be sufficiently small to minimize the insertion loss, and the resulting via diameter is 0.423 mm. However, due to fabrication constraints a value of 0.508 mm (20 mil) is considered for the via diameter and a via pitch of 0.813 mm (32 mil) is kept for the original design to ensure minimum insertion loss. The influence of the via diameter on the transmission losses in this particular case has been studied, and the results can be found in [1].

The aperture matching circuit is made of a capacitive blind via and an inductive diaphragm. The various parameters are optimized using HFSS for a waveguide with perfectly conducting vertical walls to reduce the computation time. The model is fed with a TE10 mode and radiated into free space. The best solution is obtained using a capacitive post with a 0.6 mm diameter and 1.3 mm in length placed on the centre line of the waveguide and 11.7 mm away from the aperture. The inductive diaphragm is realized with two vias 4 mm apart (centre-to-centre) placed 11.6 mm away from the aperture. This is illustrated in *Figure 2*. The return loss of the radiating waveguide with the aperture matching circuit is shown in *Figure 3*. The match is achieved in a narrow band, but it is sufficient for our application (20.2 GHz to 21.2 GHz). The complete model, including the coaxial-to-waveguide transition and the aperture matching circuit was then simulated. Results for the return loss are also shown in *Figure 3*. The impedance bandwidth is finally from 20.2 GHz to 21.3 GHz, which encloses the desired bandwidth of operation. The bandwidth limitation is due to the narrow band aperture matching circuit.

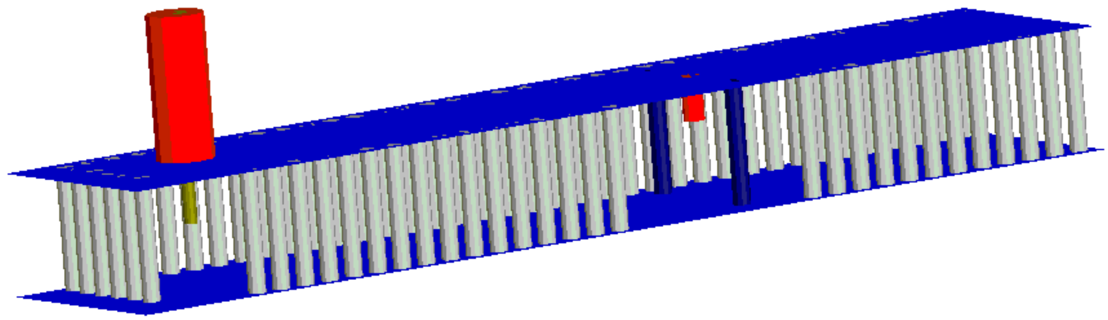

Figure 2. Laminated waveguide model

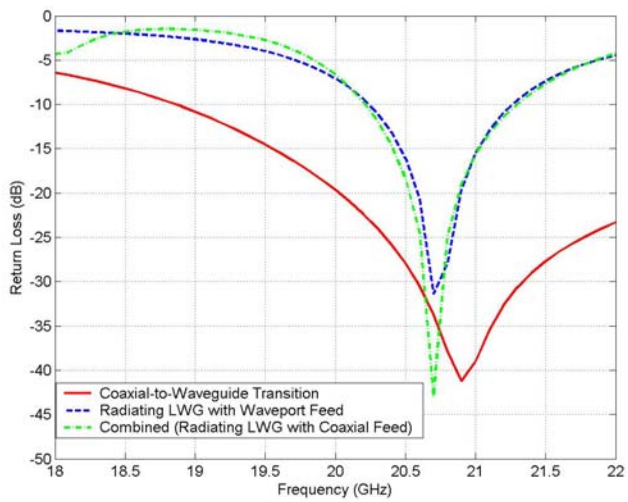

Figure 3. Return losses of the feed and aperture matching circuit and of the radiating LWG (results from [1])

A number of prototypes were fabricated to fully characterize radiating and non-radiating waveguides (*Figure 4*). The study of non-radiating waveguides is omitted in this document, but it can be found in [1]. From it, we deduced that the attenuation factor was 2.2 Np/m and the connector loss was 0.15 dB. After lamination and drilling, all of the holes, except the probe and the capacitive post holes, are plated to form vias. A pin is inserted for the probe and then the K-type connector is placed over the pin. To make the capacitive post, a pin is also inserted in the corresponding hole and is soldered to the top plate. Radiating LWGs of two different lengths were fabricated. As the aperture matching and probe transition circuits were designed independently, it is possible to lengthen the LWG without changes to the design.

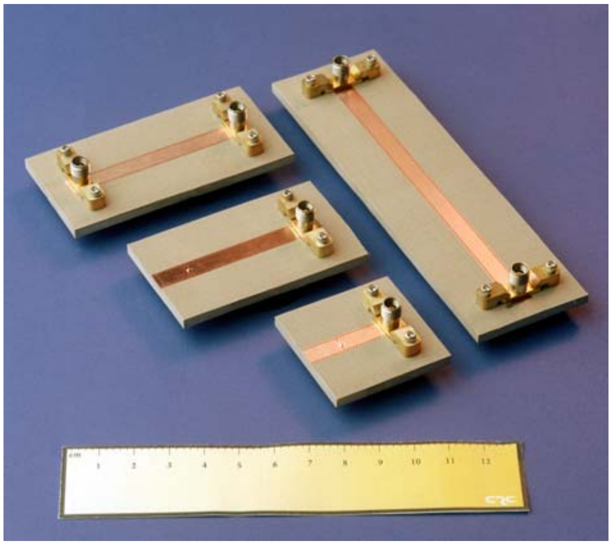

Figure 4: Laminated waveguide prototypes

The reflection coefficients of the short and long radiating LWGs are presented in *Figure 5*. The short and long prototypes have a 10-dB return loss bandwidth from 20.0 GHz to 21.0 GHz and from 20.1 GHz to 21.1 GHz, respectively. These results are slightly shifted down in frequency (about 0.5%) compared to the simulation results.

As the vias, probe and post are buried in the material they cannot be measured after fabrication with a non-destructive process. The thickness of the substrate was however measured, and its value was as expected. Prior to fabrication, various simulations were done to estimate the effect of varying the probe and capacitive stub length, as these components are subject the most to manufacturing tolerance errors. In particular, the tolerance of the drilling machine is +/-50 μm. The results of this study [1] demonstrate that a 50 μm difference in probe and/or stub length has a significant impact on the impedance match and introduces a frequency shift of the order of the one observed by measurement (0.7%). On the other hand, the probe and capacitive post diameters are well controlled in the fabrication process, and variations in the impedance characteristics due to fabrication tolerances have little effect.

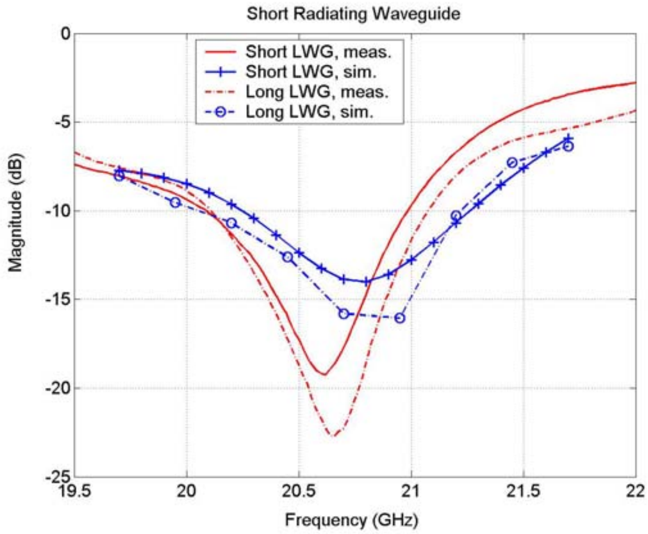

Figure 5. Simulated and measured return loss of the radiating LWGs

The radiation patterns were measured and the results for the long prototype are shown in *Figure 6*. The corresponding data obtained by simulation are also presented. Note that the K-connector feeding this radiating laminated waveguide prototype was soldered directly on top of the substrate part and not bolted. In fact, the metallic clamps drastically affect the radiation patterns in the H-plane. The measured radiation patterns correlate in both planes closely with the expected results. The half-power beamwidths are 122^{o} and 64^{o} in the E- and H-planes, respectively. The measured cross-polarisation levels are reasonably low, being 20 dB down from the co-polarisation levels. The measured maximum gain is nearly identical to the predicted one (2.7 dBi). The measured gains in both E- and H-planes in the boresight direction are different but within a 0.5 dB margin (3.1 dBi for E-plane and 2.6 dBi for H-plane). The discrepancy between the two measured gains in the boresight direction is due to the antenna measurement system. The gain obtained by simulation for the short radiating waveguide is 0.5 dBi higher than the gain for the long radiating waveguide. This is due to lower insertion loss as the waveguide is shorter.

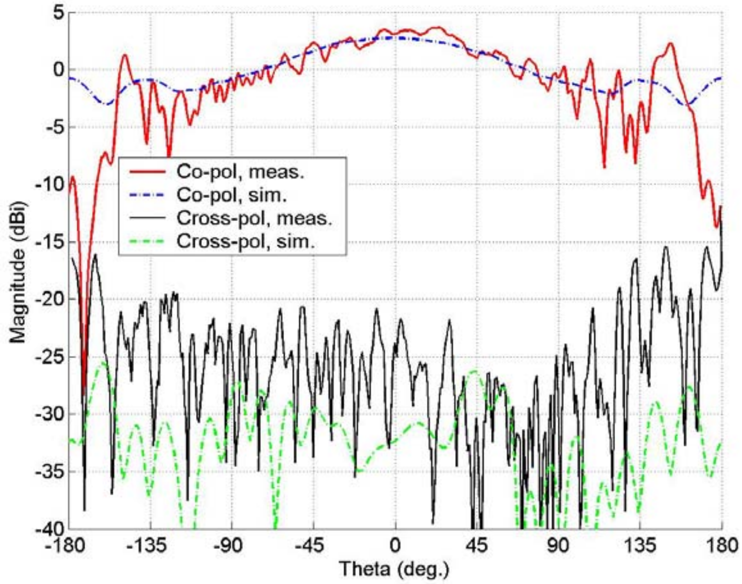

a)

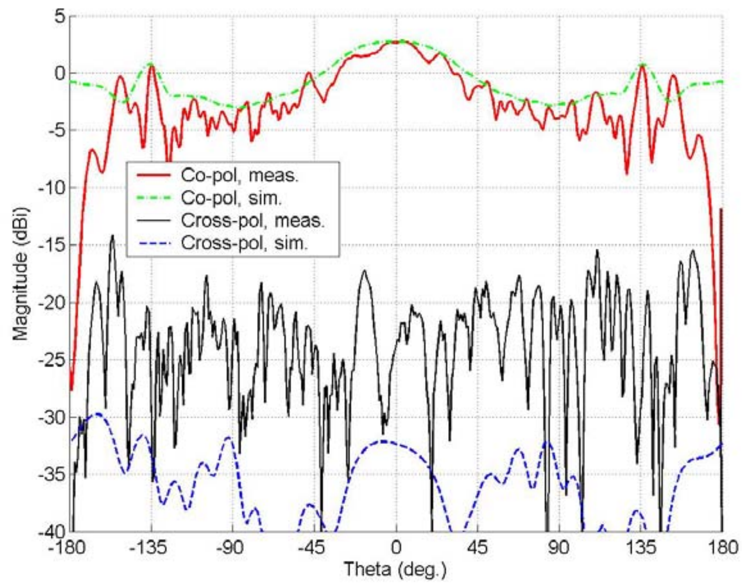

b)

Figure 6: Simulated and measured E- and H-plane radiation pattern of the long radiating LWG (results from [1])

2. Design and simulation of the five-element array

2.1 Electromagnetic model

Simulating an array of five LWG elements using HFSS is an involved problem. Although it may be possible to simulate five separate elements within one substrate, the numbers of tetrahedra forming the mesh structure required in HFSS will be impracticably large. As it has been reasonably established that a radiating RWG can approximate the input impedance and the far-field radiation patterns of a single LWG element [1], the same can be done for an array. The array is then simulated by replacing the via walls with solid walls whose thickness corresponds to the via diameter. To account for the diffraction at the edges of the elements, a round edge with the same diameter as the vias is used on all of the vertical walls at the radiating edge of the model. The elements are half a wavelength apart at the 20.7 GHz centre frequency and they are each fed by a separate coaxial line. As the physical distance between the elements is small, short and long LWGs are alternated in order to provide sufficient space for soldering the K-connectors, and to connect the test equipment. The model, presented in *Figure 7*, is simulated on a 3-by-3-inches substrate material. The array is radiating on the Z-direction. The five coaxial feeds are numbered from the left to the right. This notation is kept for the remaining of the document.

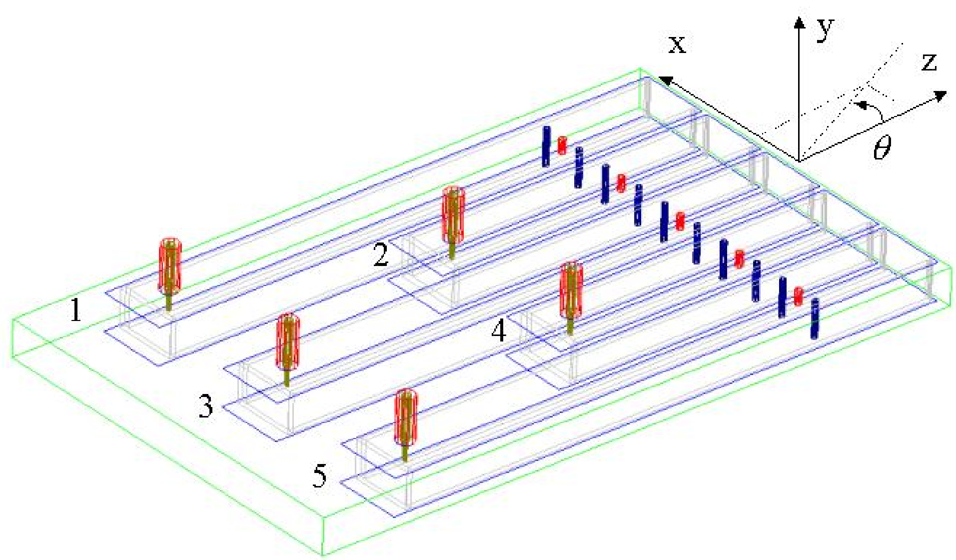

Figure 7. *The five-element array model*

The electromagnetic model was created during a previous study [1], but the results obtained by simulation showed that the developed model contained errors. It has been corrected since, and the results presented hereafter are obtained from the simulation of the updated model for the five-element array.

2.2 S-parameter Results

The S-parameter matrix of the array was simulated from 19.7 GHz to 21.7 GHz. Results in terms of input impedance, return loss and mutual coupling are presented in this section. The scan return loss, computed from the elements of the S-parameter matrix, is also discussed in this section.

2.2.1 Input impedance

Figure 8 and *Figure 9* presents respectively the input impedance for each element on the Smith chart, and the corresponding return loss. The responses for the short and long radiating LWGs are slightly different, but for all the antennas the maximum return loss is shifted to 21.1 GHz. The long radiating laminated waveguides have a good match from 20.3 GHz to 21.5 GHz and the short ones are matched from 20.5 GHz to 21.5 GHz.

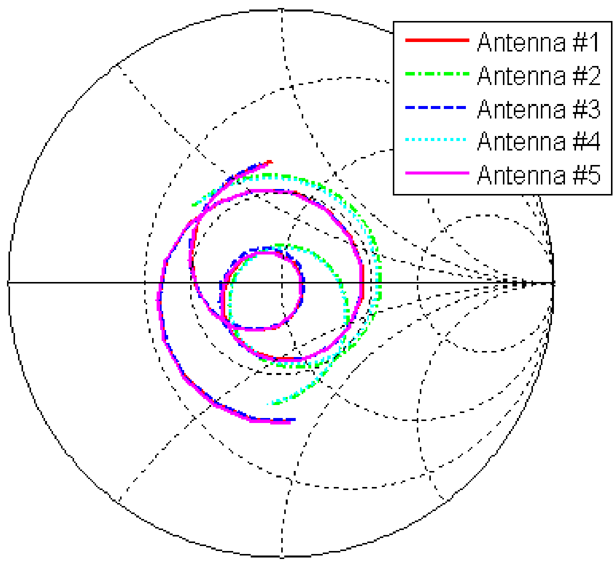

Figure 8. *Input impedance and return losses of the five radiating LWGs*

On the Smith chart representation, one can notice that the loops are centered on 50 Ω (centre of the chart) and they are smaller for the long LWGs, thus providing a good match over a larger frequency band. The response for the long LWG in the centre of the array (Antenna #3 in *Figure 8* and *Figure* 9) is slightly different than the response of the two long LWGs located on each side of the array due to a stronger coupling effect. The differences between the responses of the two short LWGs and the difference between the responses of the two long LWGs on the array side are introduced by the asymmetrical meshing of the model.

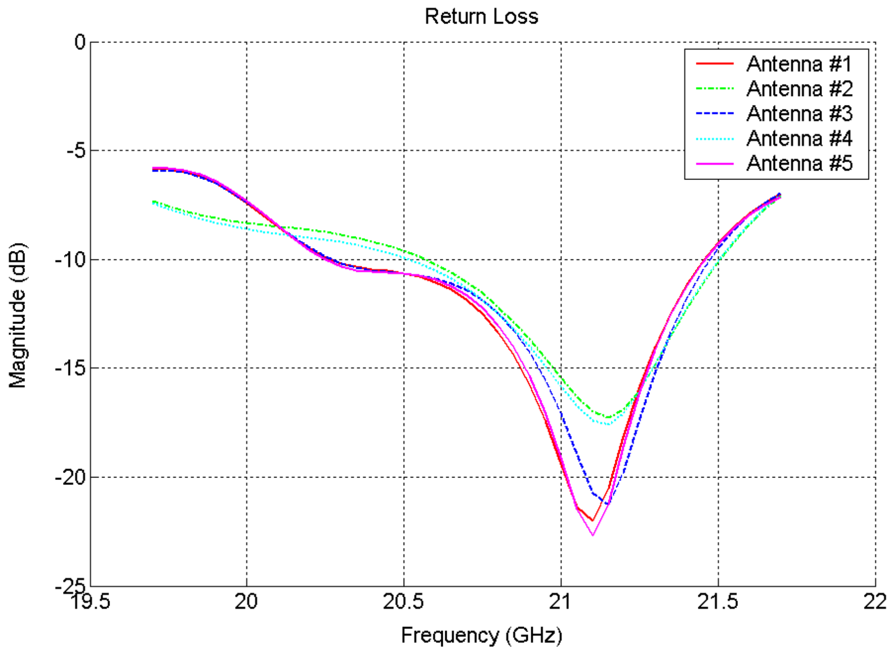

Figure 9. *Input impedance and return losses of the five radiating LWGs*

For comparison, *Annex 1* provides the results for arrays of five short LWGs and five long LWGs. The return loss responses are similar to these ones.

2.2.2 Mutual coupling

The mutual coupling, presented in *Figure 10*, indicates that the maximum coupling between two adjacent elements over the bandwidth is lower than –18 dB. The coupling decreases by about 10 dB when the considered elements are separated by one other element, and by about 20 dB when separated by two other elements. Note that the mutual coupling between the short elements (S42 in *Figure 10*) is 1 dB higher than the mutual coupling between the long element on the array sides and the long element on the centre (S31 and S53 in *Figure 10*).

For comparison, *Annex 1* provides the results for arrays of five short LWGs and five long LWGs. The coupling responses for the array of five short LWGs are similar. The responses for the array of five long LWGs are more constant over the frequency band, and remain below -20 dB between two consecutive elements.

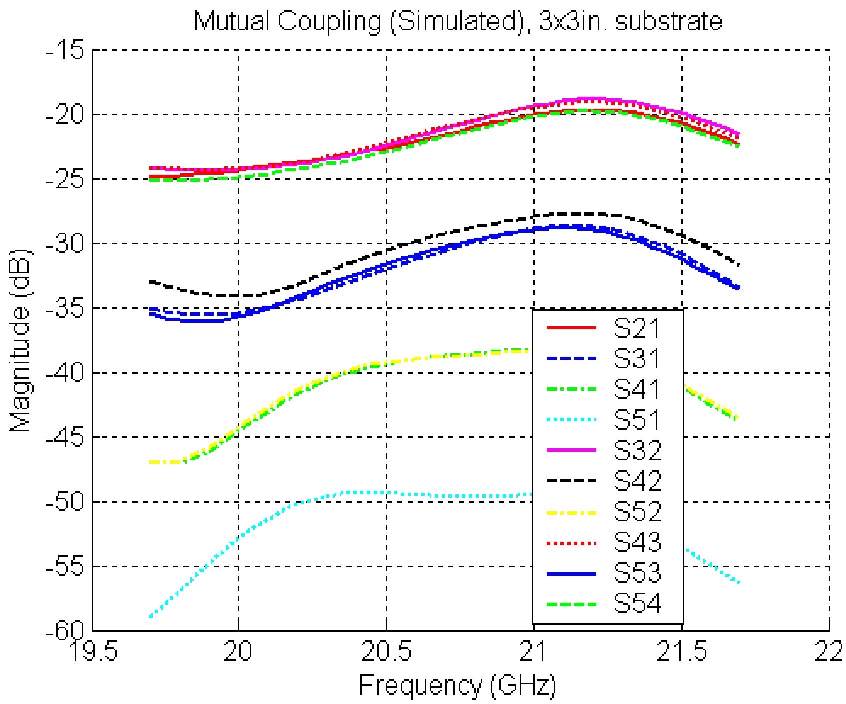

Figure 10. *Mutual coupling between the five radiating LWGs*

2.2.3 Scan impedance

When the radiating elements are used in a phased array, a characteristic of interest is the scan input impedance of each element, or the corresponding scan return loss. Due to the mutual coupling the return loss of an element depends on the scan angle when all the elements are excited. This "active impedance", also called scan impedance, can be calculated from the S-parameter matrix of the array. For a linear array with uniformly spaced elements, the scan impedance is given by the formula:

$$Sscan_{ii}(\theta_o) = \sum_{m=1}^{N} S_{mi} \frac{A_m}{A_i} e^{(\phi_m - \phi_i)} e^{-jkd(m-i)\sin(\theta_o)} \tag{1}$$

where

- N is the number of elements of the array,
- d is the inter-element spacing,
- k is the wavenumber,

- θ_o is the scan angle,
- A_i is the amplitude weighting of the element i, and
- ϕ_i is the phase weighting given to the element i.

The results of the scan impedance at 20.7 GHz for each element are given in *Figure 11*. The mutual coupling actually improves the return loss (RL) for a 0^o scan angle. Note that the side elements have the highest RL for this value because they have only one neighbour element. The RL reaches the -10 dB level for a 34^o scan angle for element #5, 36^o for element #4, 40^o for element #2, 43^o for element #3 and 68^o for element #1. The maximum RL remains below -6 dB for element #2, 3 and 4, and below -8 dB for element #1 and 5. We can consider a 0.5 to 1 dB gain decrease for scan angles higher that 40^o.

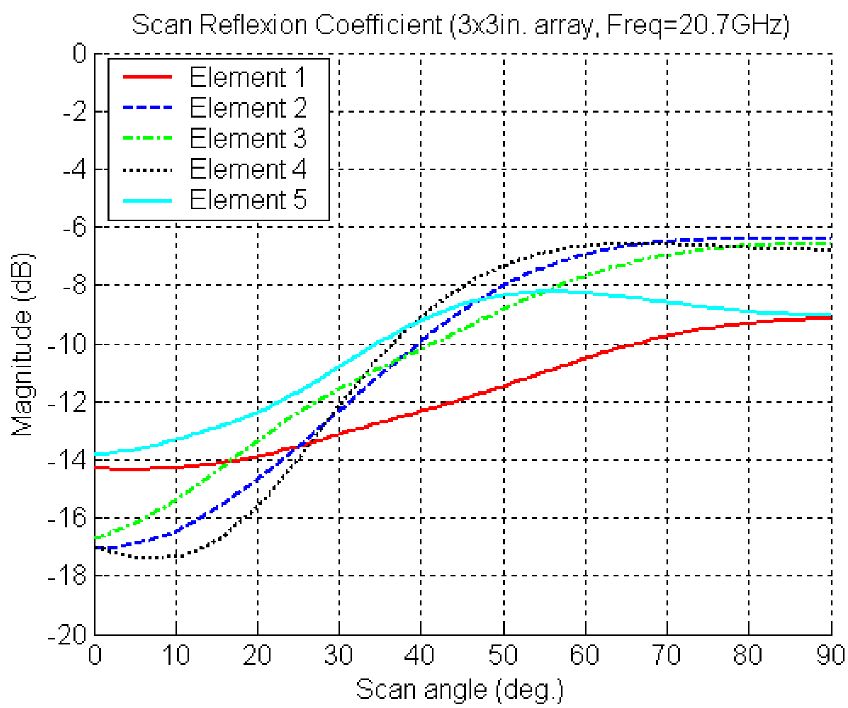

Figure 11. *Scan return loss of the five radiating LWGs at 20.7 GHz*

2.3 Radiation patterns

The radiation patterns for the array are simulated with HFSS for various configurations. Firstly, the far-field patterns are computed for a boresight radiation for several frequencies, and the results are analyzed. Secondly, the patterns are computed for several scan angles for different frequencies, and the main characteristics are extracted. But as the array is composed of laminated waveguides of different lengths, the phase of the excitation must be compensated for. An investigation is then carried out to find the best phase coefficients for maximizing the antenna gain at the centre frequency. The results of this investigation are presented in the following section.

2.3.1 Excitation coefficients

As mentioned previously, the length difference between the short and long waveguides must be compensated for in phase to achieve proper array radiation patterns. The phase compensation was evaluated in [1] by only considering the length difference between the short and long LWG. The authors ended up with a -171^{o} phase difference. We investigated this aspect further using our numerical model. A phase difference of -188^{o} is then optimized by simulation observing the wave front at the waveguide apertures at the 20.7 GHz centre frequency. In addition, the long laminated waveguide at the centre of the array needs to be fed with a 5^{o} phase difference compared to the phase of the outer long laminated waveguides. One anticipates that this phase difference is to compensate for the mutual coupling effect. The electrical field propagation in the waveguides for the initial and optimized phase excitations are shown in *Figure 12*.

Phase excitation:

- Long LWGs: 0 deg.
- Short LWGs: -171 deg.

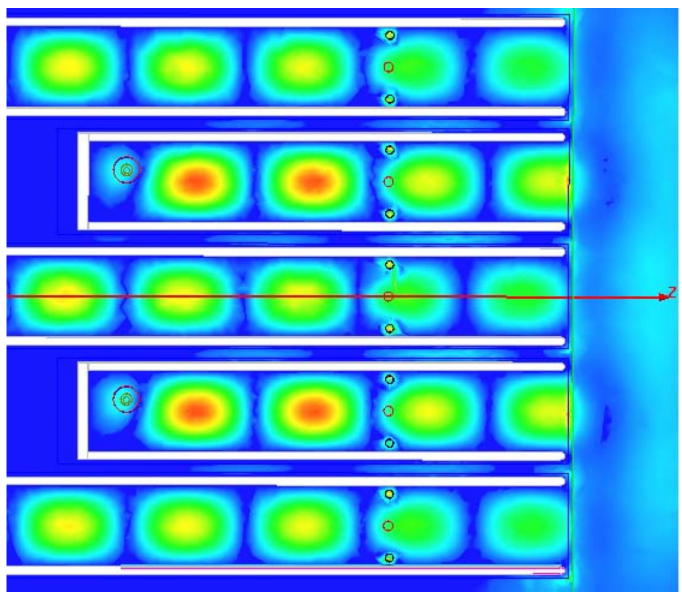

Figure 12a. E-field propagation in the waveguides for the initial phase excitation

The amplitude excitation of all the elements is unity.

Phase excitation:

• Side Long LWGs: 0 deg.

• Centre long LWG: 5 deg.

• Short LWGs: -188 deg.

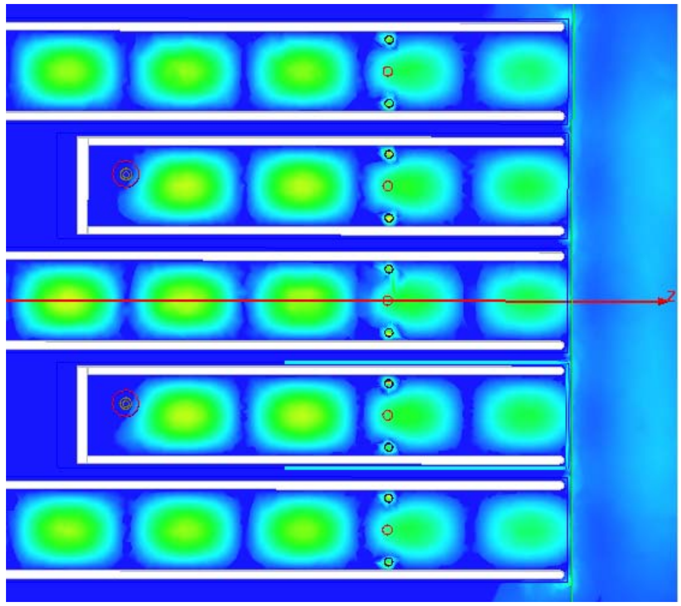

Figure 12b. *E-field propagation in the waveguides for the optimized phase excitation*

2.3.2 Boresight radiation patterns

The radiation patterns are computed for various frequencies in the band of interest (20.2 GHz to 21.2 GHz), and are shown in *Figure 13*. They are quite stable over the bandwidth. The high level lobes occurring between +/-100 ^{o} to +/-120 ^{o} are due to the diffraction at the edges of the dielectric material. A maximum gain of 9.7 dBi is reached at the centre frequency. Note that the gain calculated from the array theory considering the gains at 20.7 GHz of the short and long elements (3.25 dBi and 2.7 dBi, respectively) reaches 9.9 dBi. The gain decreases when the frequency moves away from the centre frequency because the optimum phase weighting at 20.7 GHz is kept for computing the radiation patterns at other frequencies. The half-power beamwidth (HPBW) is about 20 ^{o} to 22 ^{o}. The first sidelobe levels (SLLs) are lower than -13.2 dB all over the frequency band. The cross-polarization level in the boresight direction is lower than –40 dB across the frequency band. These characteristics are summarized in *Table* 1.

For comparison, *Annex 1* provides the results for arrays of five short LWGs and of five long LWGs. The maximum gain is 0.4 dB higher for the array of short LWGs due to less transmission loss. The half-power beamwidths are comparable, and the cross-polarization is slightly lower for the array of long radiating laminated waveguides.

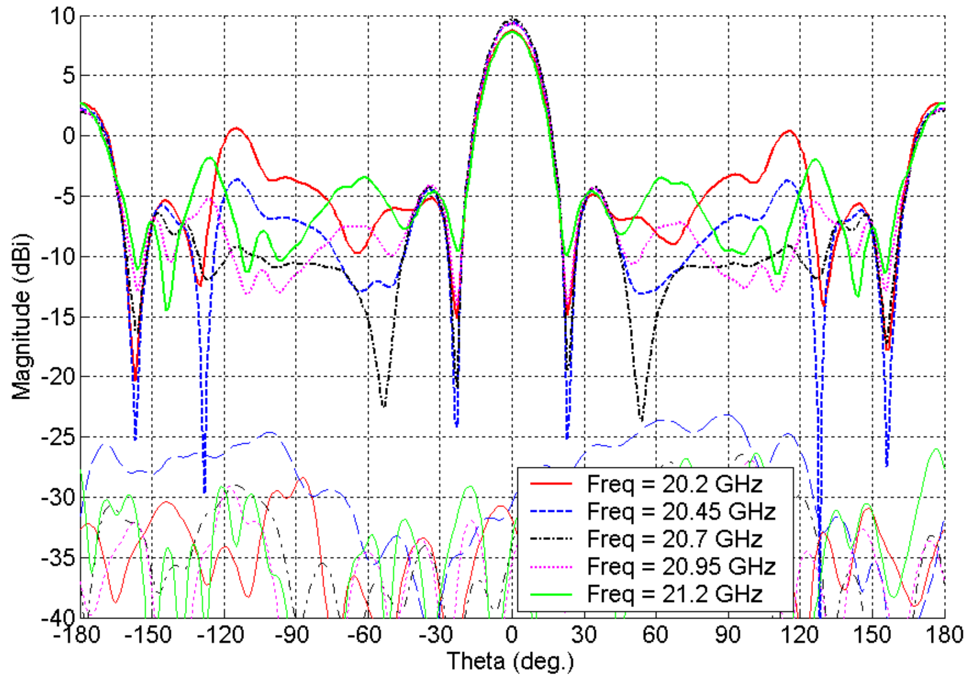

Figure 13. *Boresight co- and cross-polarisation radiation patterns at several frequencies*

Table 1. *Simulated H-plane boresight radiation characteristics of the five-element array*

Freq. (GHz)	Gain (dBi)	HPBW (deg.)	SLL (dB)
20.2	8.7	22	-13.5
20.45	9.4	22	-13.8
20.7	9.7	22	-13.9
20.95	9.4	20	-13.5
21.2	8.7	20	-13.2

2.3.3 Scanned radiation patterns

As this array is designed for use as an antenna of a phased array, scanned radiation patterns are simulated as well. The phase of each element is adjusted at the 20.7 GHz centre frequency to steer the main beam from 0° to 60° with 10° steps. The phase excitation for each element is given in *Table 2* for several scan angles. The amplitude excitation of all the elements remains unity.

__Table 2.__ Phase excitations for various scan angles

Scan angle (deg.)	Phase excitations (deg.)				
	Element #1	Element #2	Element #3	Element #4	Element #5
0	0	-188	5	-188	0
10	0	-157	67	-94	125
20	0	-126	128	-3	246
30	0	-98	185	82	360
40	0	-72	236	159	463
50	0	-50	281	226	552
60	0	-32	317	280	624

The scan radiation patterns obtained by simulation are shown in *Figure 14*. The maximum gain decreases by 3.2 dB from the boresight direction to a 60 ^{o} scan angle. The HPBWs fluctuate between 21 ^{o} and 29 ^{o}. The maximum side lobe level remains below -9.2 dB from the maximum gain over the considered scan angle range. These characteristics are summarized in *Table 3*. Note that a beam squint occurs for scan angle from 20^{o}, due to the coupling between the radiating elements.

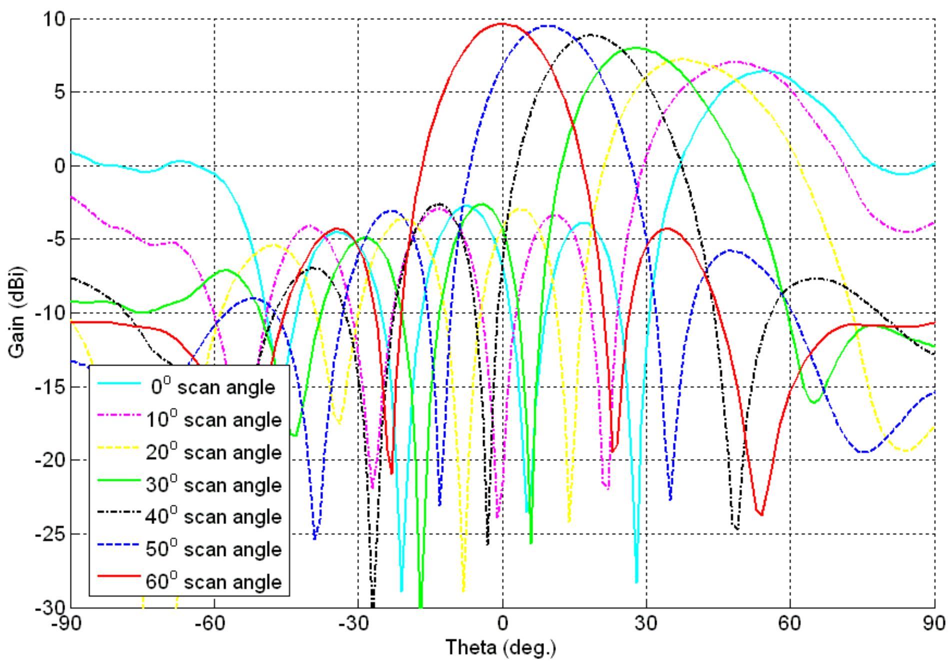

__Figure 14.__ Scanned radiation patterns of the five-element array

Table 3. *Simulated H-plane scanned radiation characteristics of the five-element array at 20.7 GHz*

Scan angle (deg.)	Angle at max. gain (deg.)	Gain (dBi)	HPBW (deg.)	SLL (dB)
0	0	9.7	22	-13.9
10	10	9.5	22	-12.5
20	19	8.8	22	-11.4
30	28	8.0	24	-10.6
40	37	7.2	28	-10.2
50	49	7.0	29	-9.9
60	55	6.4	27	-9.2

Note: The radiation patterns are evaluated every degree

3. Measurement and Analysis

Two prototypes (Array D and Array E) were fabricated for validating the results obtained by simulation. Each element of the arrays is fed through a K-connector soldered on top of the waveguide, as illustrated in *Figure 15*. For both prototypes the array is realised on a 3 by 3 inches CLTE substrate.

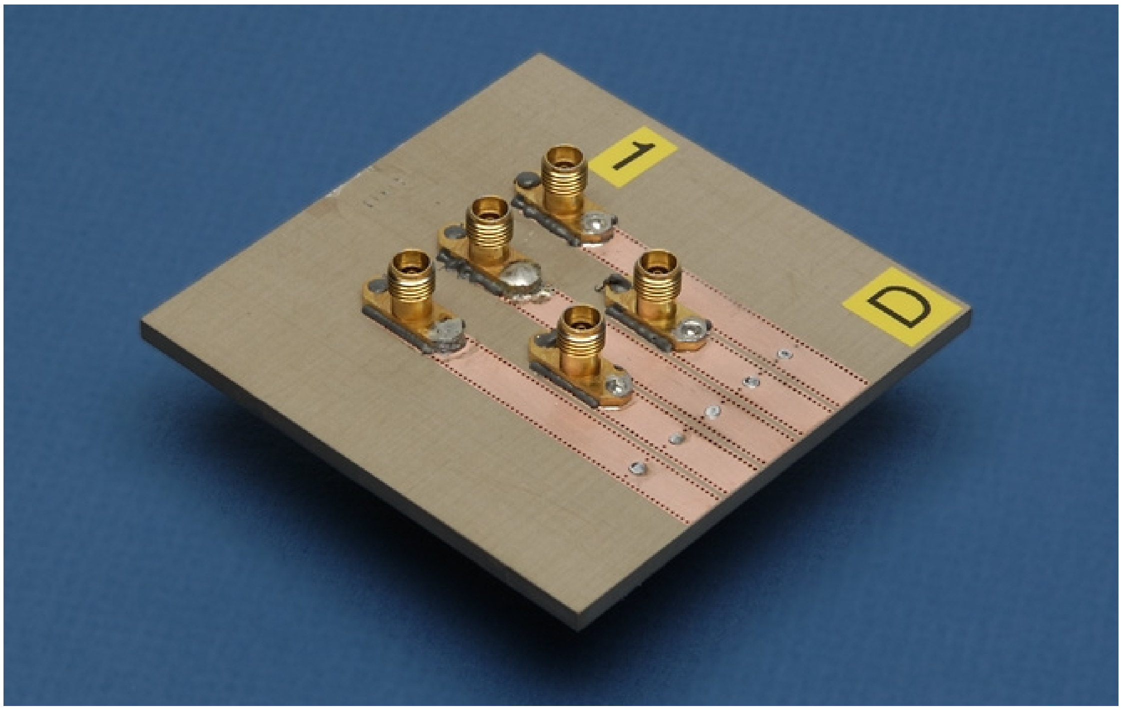

Figure 15. *Picture of the five-element array prototype*

The input impedance and the coupling between the elements were characterised by measurement of the S-parameter matrix with a vector network analyser (VNA). Measurement of the radiation patterns in the boresight direction and for several scan angles for various frequencies were carried out at the CRC antenna facilities. The results are compared with the simulation, and are presented in this section.

3.1 S-parameter results

The S-parameter matrix of the two prototypes was measured with a Wiltron 360B VNA. The results are reported and analysed below.

3.1.1 Input impedance

The input impedance for the five elements of the arrays E and D on the Smith Chart representation is shown in *Figure 16*, and the corresponding return losses are presented in *Figure 17*. The elements do not show the same match.

a) Array D

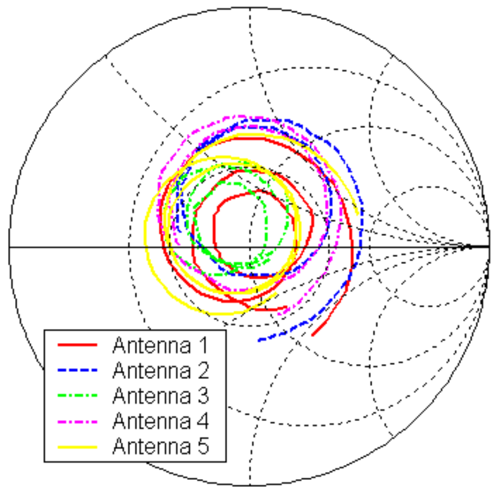

b) Array E

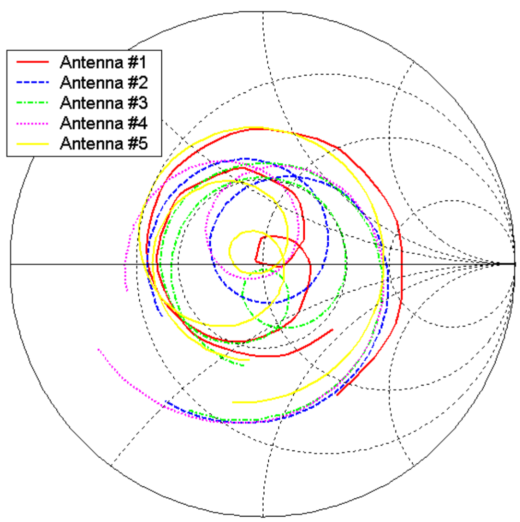

Figure 16. *Input impedance of the radiating LWGs of a) Array D and b) Array E*

For array D, one notices from the Smith chart representation (*Figure 16a*) that the input impedance forms a large loop around the centre (50Ω) for antenna #2, #4 and #5, which indicates a good match over one or two narrow frequency bands. This is confirmed in *Figure* 17*a* that represents the return loss of each antenna element. Elements #1 and #3 show a good match over the largest band (20.1-21.2 GHz and 20.1-21.4 GHz, respectively) and elements #2 and #4 (short LWGs) present the narrowest band (20.45-20.9 GHz). Element #5 is matched in two frequency bands (20.15-20.6 GHz and 21-21.5 GHz).

For array E, the input impedance forms a smaller loop (close to 50Ω) for all the elements (*Figure 16b*). The minimum return losses of elements #1 and #4, as numbered in *Figure 7* page 8, occur at the same frequency (20.5 GHz) and those of elements #2 and #3 occur at 20.6 GHz. Element #5, at the far right side of the array, exhibits the largest bandwidth (20-21 GHz), as shown in *Figure* 17*b*. The discrepancies in matching are due to a slight variation in probe and/or stub length, as mentioned for the single radiating laminated waveguide [1]. Overall, the elements are matched from 20.3 GHz to 20.85 GHz.

a) Array D

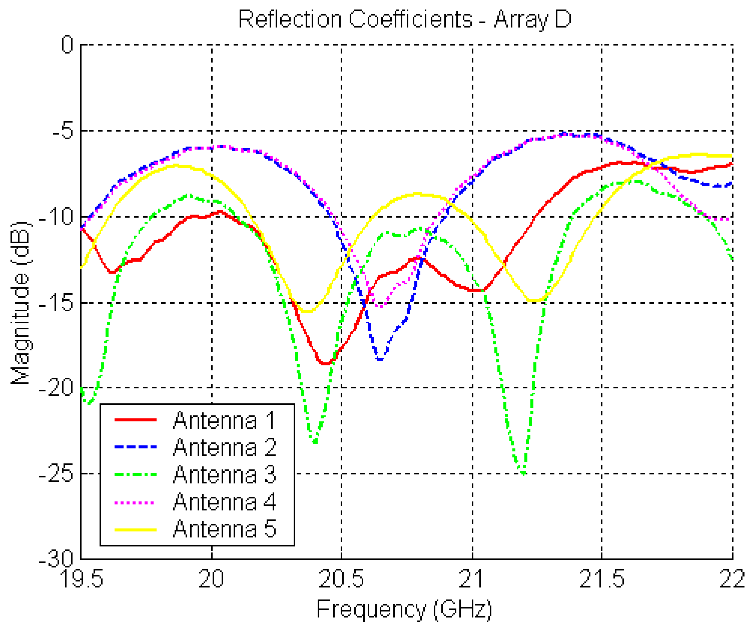

b) array E

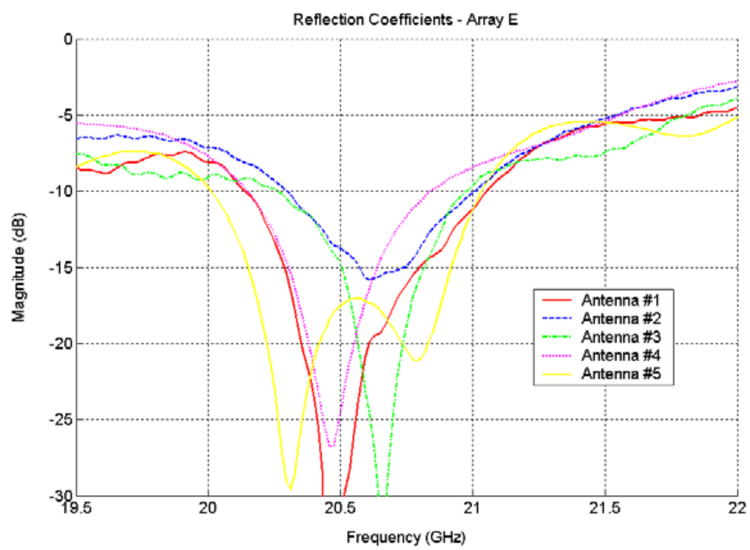

Figure 17. *Return loss of the radiating LWGs of a) Array D and b) Array E*

3.1.2 Mutual coupling

The mutual coupling between antenna elements for arrays D and E is shown in *Figure 18*. Results for both arrays are similar. The mutual coupling indicates that the strongest coupling, which occurs between two adjacent elements, is lower than –20 dB over the bandwidth. The coupling decreases by about 10 dB when the considered elements are separated by one other element, which corroborates the results obtained by simulation. The measurements agree quite well with the simulation results.

a) Array D

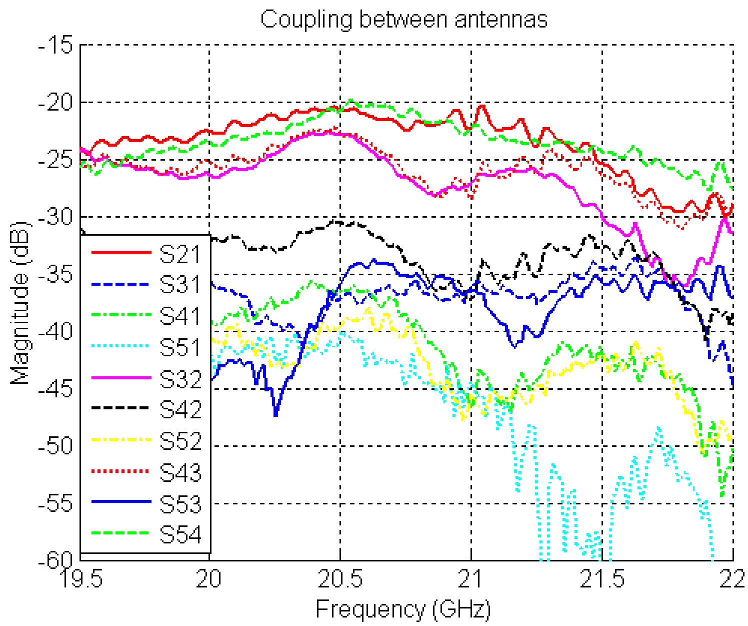

b) Array E

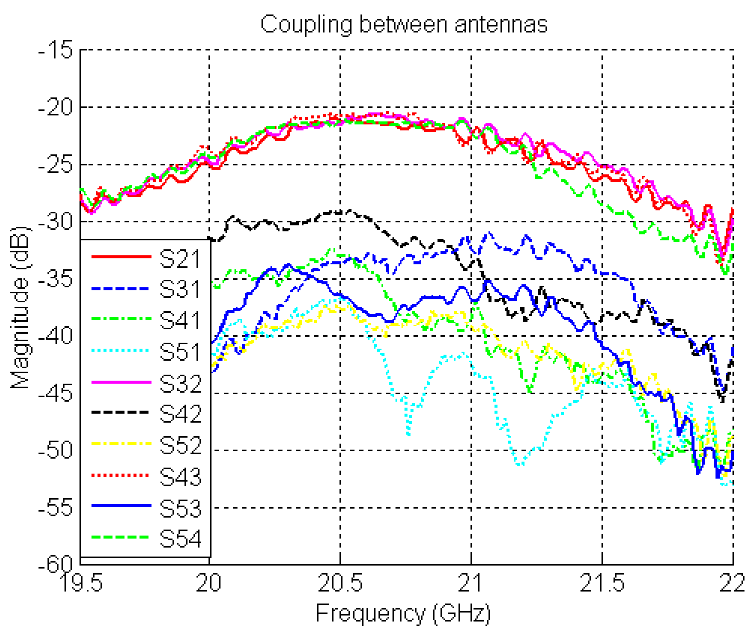

Figure 18. *Mutual coupling between of the radiating LWGs of a) Array D and b) Array E*

Comparing the results of the S-parameters of the two arrays, it appears that the antenna elements of array E exhibit a better match in the operating frequency band. This array was then chosen for measuring the radiation patterns. A feeding system is required to properly excite the five elements. The next section presents the characterization of the various components of this system used for measuring boresight and scan radiation patterns.

3.2 Radiation pattern measurement setup

As mentioned previously, the length difference between the short and long waveguides must be compensated for in phase to achieve proper array radiation patterns. A feeding system was then setup. The system includes an eight-way power divider (the three unused output were terminated with 50 Ohms), line stretchers used to adjust the phase excitation of each element, and phase-stable flexible cables of equal length to connect the line stretchers to the antenna coaxial feeds, and 90^{o} bends. Each individual component was measured (*Figure 19*). The components were then selected to minimize, at the centre frequency and over the operating band, the discrepancies in phase and magnitude of the five feed lines. The measurements of all the components are provided in *Annex 2* to *Annex 5*, and the results are summarized in this section.

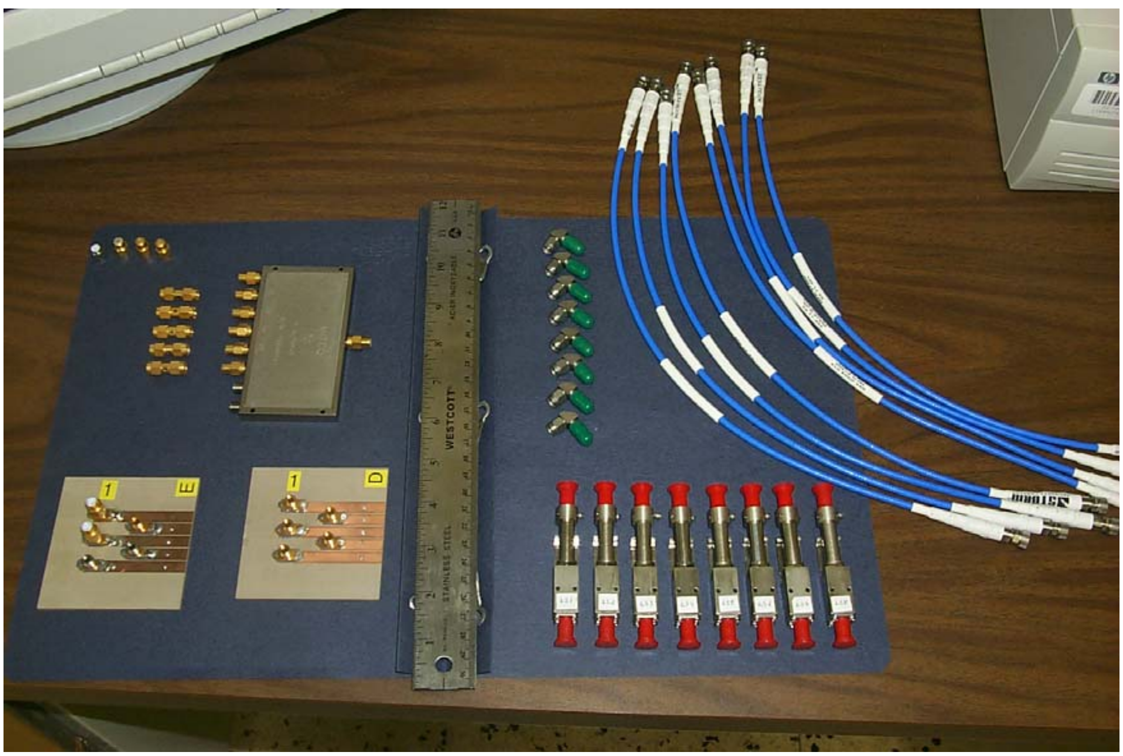

Figure 19. *LWG arrays and components of the feeding system*

3.2.1 Power divider

The eight-way power divider was characterized between 19.5 and 22 GHz. The measurements of the return loss (RL), transmission factor, in magnitude and phase, and the coupling are provided in *Annex 2*. The results are summarized below.

As expected, all the ports (input port 0 and output port 1 to 8) have a good match over the frequency range of interest. In the 20.2-21.2 GHz band, outputs #3 and #5 have the worst RL. Output #5 has the highest insertion loss (IL) at 20.7 GHz and the highest IL variation over the band (11.45 dB and 0.95 dB, respectively). The phase difference of the transmission factor is less than 5^o all over the operating band. The coupling between outputs was also measured. Most of the coupling coefficients are below -30 dB. The worst coupling coefficients are between outputs#1 and #2, #3 and #4, #5 and #6, and #7 and #8, probably due to the structure of the power divider.

3.2.2 Line stretchers

The line stretchers are passive components used to introduce a phase shift that can be adjusted manually. Each is composed of fix and mobile parts. The phase is adjusted by extending the line length. The translation is obtained by rotating the mobile part. The full variation is realised by 18.5 turns.

The eight line stretchers were measured for several configurations. The results are provided in *Annex 3* and are summarized below. The S-parameter matrix was evaluated for the short and long positions. The short position corresponds to the shortest line length (therefore the smallest phase shift) and the long position corresponds to the longest line length (the largest phase shift). The phase shift of one line stretcher was measured for every turn from the short to the long positions. The length variation is about 23mm.

All the line stretchers are well matched, as the return loss measured for both ports of each component is lower than -18.5 dB over the frequency range of interest, for both the short and long positions. The insertion loss is consistent between the line stretchers, and its average over the frequency range is about 0.35 dB for the short position, and 0.45 dB for the long position. The maximum difference of insertion loss between the eight line stretchers is 0.2 dB, and it is only 0.1 dB at 20.7 GHz. The phase is consistent between the line stretchers, as the difference over the frequency range is lower than 10^o for the short and long positions. In both extreme positions, the phase variation versus frequency is uniform, and the difference between the line stretchers is quite constant.

The S-parameters of line stretcher #1 were measured for every turn from the short to the long position. The return loss varies significantly and not uniformly, but the line stretcher remains well matched for all the turns over the frequency range. The maximum insertion loss variation is lower than 0.2 dB over the frequency range. The phase varies linearly, with a 20^o step per turn at 20.7 GHz except for the first turn where the phase variation is 11^o and the incomplete last turn where the phase variation is 9^o.

3.2.3 Phase-stable cables

To ensure phase stability in transmission, phase-stable cables are used for the setup. Eight cables were measured. The results are provided in *Annex 4* and are summarized below.

As expected the eight cables are well matched. Cable #4, however, exhibits a higher return loss than the other cables. The insertion loss are similar, and their average over the frequency range is 0.95 dB. The phase of the transmission factor varies considerably from one cable to another, probably due to slight length difference. The difference remains quite constant versus frequency. The phase stability of the cables was also verified for several bends: a bend lower than 90^o, a360^o bend (one loop) and a 450^o bend ($1^{1/4}$ loop). The variations of the return loss, insertion loss and transmission factor phase are negligible. We can then bend the cables as required without further calibration.

3.2.4 Ninety-degree bends

Ninety-degree bends are used to ease the connection between the line stretchers and the array elements through the flexible phase-stable cables. Eight ninety-degree bends were measured. The results are provided in *Annex 5* and are summarized below.

The return losses of the eight bends are below -20 dB over the frequency band. The measurement of the transmission factor shows an averaged insertion loss of 0.2 dB. Some discrepancies occur between the bends. Bend #7 exhibits the lowest insertion loss (0.175 dB) at 20.7 GHz and bend #1 the highest insertion loss (0.28 dB) – see *Table 15* in *Annex 5*. At 20.7 GHz the transmission factor phase of the eight bends varies between 113^o to 122^o.

3.2.5 Complete setup

The various components were chosen and combined to reduce discrepancies in magnitude and phase between the feed lines. Two setups were used for measuring the radiation patterns, as shown in *Figure 20* and in *Figure 21*.

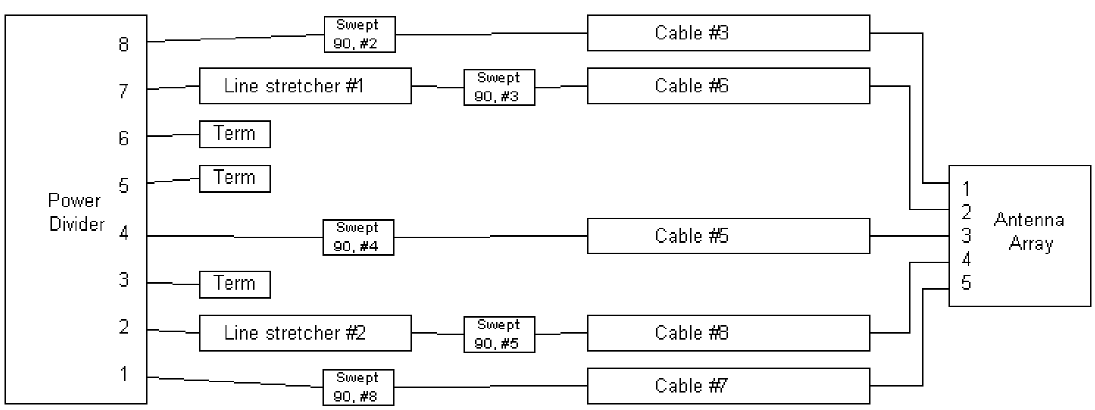

Figure 20. *Feeding system setup for boresight radiation pattern measurement*

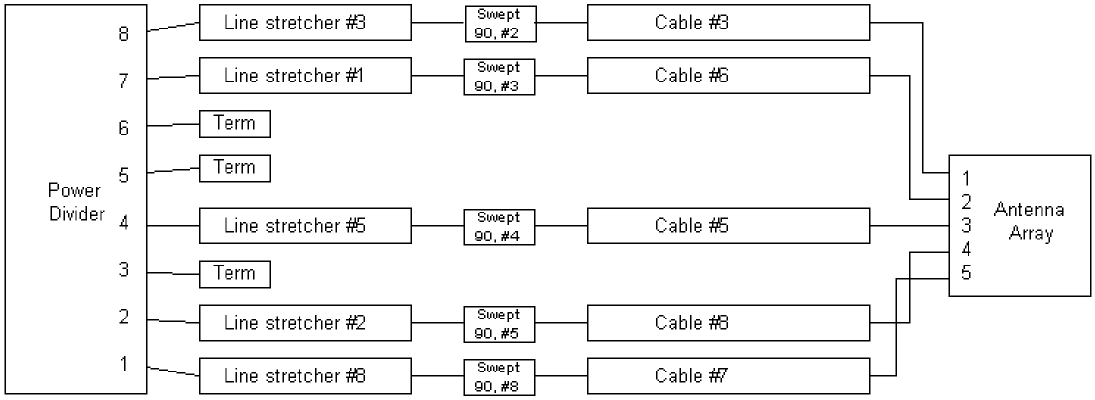

Figure 21. *Feeding system setup for scanned radiation pattern measurement*

The first setup uses two line stretchers inserted in the feed lines for the short radiating elements. This setup was used for measuring the broadside radiation patterns. The length of the line stretchers was adjusted to compensate for the length difference between the short and long laminated waveguides at the centre frequency, as it was estimated during the simulation (*Table 4*). Even though the phase setting is set correctly at the centre frequency, it does not correspond to the desired (theoretical) phase setting elsewhere (*Table 5*). The broadside radiations patterns obtained with this setup are nevertheless provided for several frequencies.

Table 4. *Magnitude and relative phase settings at 20.7 GHz for broadside radiation pattern measurement*

	Magnitude and relative phase excitations (dB and deg.)				
	Element #1	**Element #2**	**Element #3**	**Element #4**	**Element #5**
Optimum phase setting	0.0	-188.0	-5.0	-188.0	0.0
Phase (deg.)	0.0	-185.7	-6.8	-188.0	-0.7
Insertion Loss (dB)	-12.4	-12.8	-12.4	-13.0	-12.3

Table 5. *Variation of the relative phase settings for the short LWGs for broadside radiation pattern measurement at various frequencies with setup #1*

	Relative phase excitations (deg.)				
Frequency (GHz)	**20.2**	**20.45**	**20.7**	**20.95**	**21.2**
Optimal	183.5	185.7	188.0	190.3	192.5
Measured	114.0	152.9	188.0	225.7	259.6

The insertion loss of each of the five channels was measured after phase calibration. The mean insertion loss is 12.6 dB and its standard deviation is 0.3. Note that feed lines with larger loss are associated with short LWG to compensate for the difference in propagation loss between the long and short LWGs. The total decrease in level due to the insertion loss that should be taken into account in the evaluation of the measured gain is –5.5 dB.

A second setup uses five line stretchers, one for each feed line. It is used for measuring scan radiation patterns. A picture of this complete setup connected to the array antenna is shown in *Figure 22*. The phase settings were adjusted at the centre frequency for two different scan angles, 20^o and 30^o (*Table 6*). The insertion loss of each of the five channels was measured after phase calibration. For a 20^o scan angle, the mean insertion loss is 12.8 dB and its standard deviation is 0.16. The total decrease in level due to the insertion loss that should be taken into account in the evaluation of the measured gain is –5.8 dB. For a 30^o scan angle, the mean insertion loss is 12.95 dB and its standard deviation is 0.56. The total decrease in level due to the insertion loss that should be taken into account in the evaluation of the measured gain is –5.9 dB.

Table 6. *Magnitude and relative phase excitation setup for 20^o and 30^o scan angles at 20.7 GHz*

Scan angle (deg.)	**Magnitude and relative phase excitations (dB and deg.)**				
	Element #1	**Element #2**	**Element #3**	**Element #4**	**Element #5**
20 deg. (theory)	0	-126.0	128.0	-3.0	246.0
Phase (deg.)	0	-126.9	127.7	-3.4	246.1
Mag. (dB)	-13.0	-12.9	-12.6	-12.9	-12.8
30 deg. (theory)	0	-98.0	185.0	82.0	360.0
Phase (deg.)	0	-98.2	179.9	82.5	0.7
Mag. (dB)	-13.15	-12.35	-12.7	-13.8	-12.7

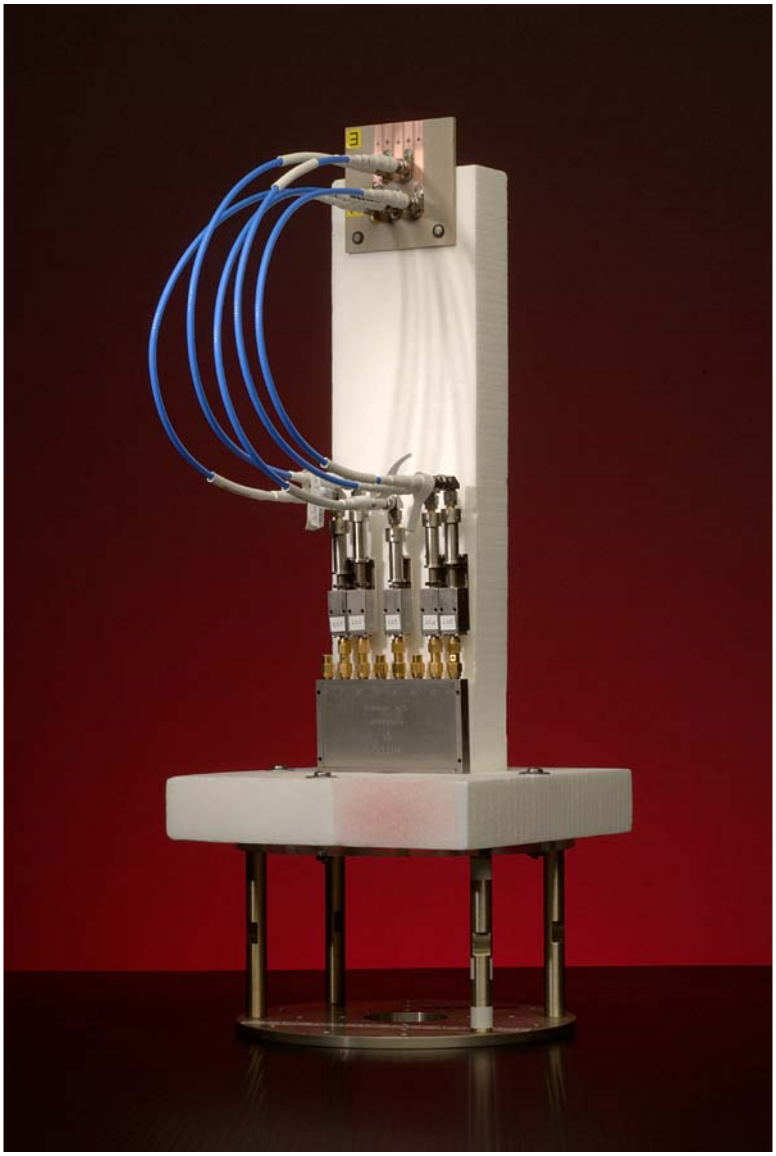

Figure 22. *Picture of the LWG array and its feeding system setup*

3.3 Boresight radiation patterns

The co-polar radiation patterns were measured for several frequencies at CRC. *Figure 23* shows the patterns for three significant frequencies in the H-plane. A gain drop of 1.0 to 1.5 dB occurs in the boresight direction for the three frequencies. This gain drop measured at 20.2 GHz and 20.45 GHz increases to 5 dB. This is due to the fact that the phase excitation setting is not optimum for all the frequencies. A maximum gain of 3.7 dB is measured at 20.7 GHz, which corresponds to a 9.2 dBi gain for the array by itself. This result is in good agreement with the prediction (9.7 dBi) allowing for a reasonable error margin in the gain calibration. The best response is obtained at 21.2 GHz. The maximum gain at 21.2 GHz is 10.1 dBi. The half-power beamwidth is 16.5° and the sidelobe levels are 13.7 dB below. The cross-polarisation is higher than predicted, but remains 25 dB below the maximum gain across the half-space. The radiation characteristics for five frequencies across the operating frequency range are summarized in *Table 7*.

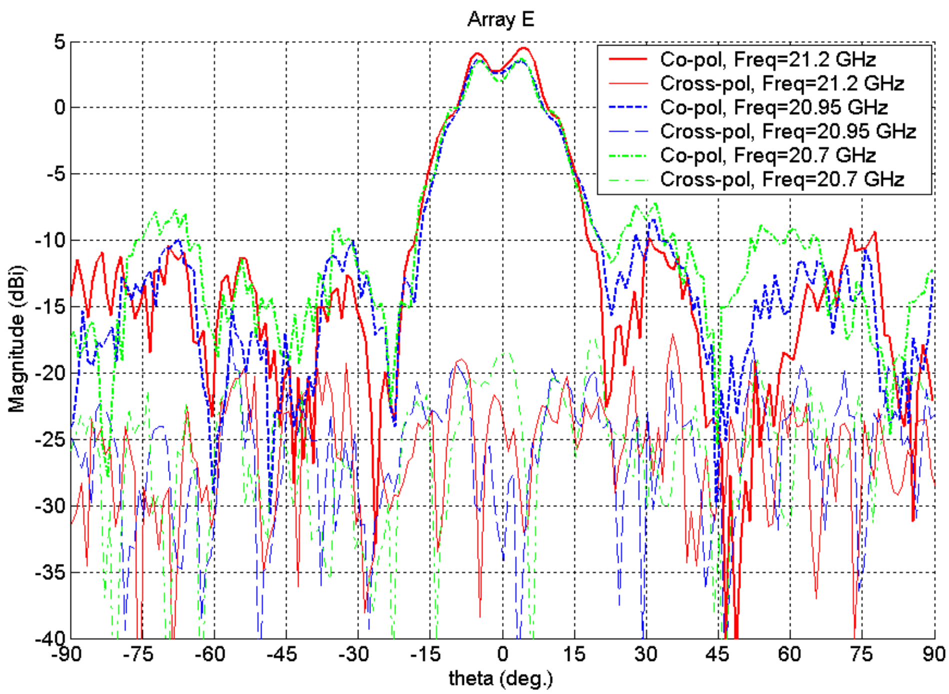

Figure 23. *Boresight radiation patterns of the five-element array for several frequencies*

Table 7. *Boresight radiation pattern characteristics of the five-element array for several frequencies*

Freq. (GHz)	Gain (dBi)	HPBW (deg.)	SLL (dB)
20.2	9.1	18.5	-8.6
20.45	9.7	16.3	-9.2
20.7	9.2	16.0	-11.0
20.95	9.1	16.5	-12.0
21.2	10.1	16.5	-13.7

Note: an adjustment of 5.5 dB corresponding to the insertion loss introduced by the feed system was made

3.4 Scanned radiation patterns

Scanned radiation patterns were also measured for several scan angles and frequencies. Results for five frequencies and for a 20 ° scan angle, are shown in *Figure 24*. The phase excitations were set according to the phase weightings provided in *Table 6*. The best radiation pattern is obtained at 20.2 GHz. The gain reaches 7.4 dBi after taking into consideration the 5.8 dB feed system insertion loss. This is only 0.4 dB less than predicted by the simulation. The radiation characteristics start to degrade when the frequency increases, as the secondary lobe around -40 ° elevation angle increases. The sidelobes, however, remain at an acceptable level up to 20.7 GHz (see *Table 8*). Note the beam squint due to the mutual coupling. The obtained scan angle is about 16-17 °. The phase excitation is an important consideration when measuring the radiation patterns for this array.

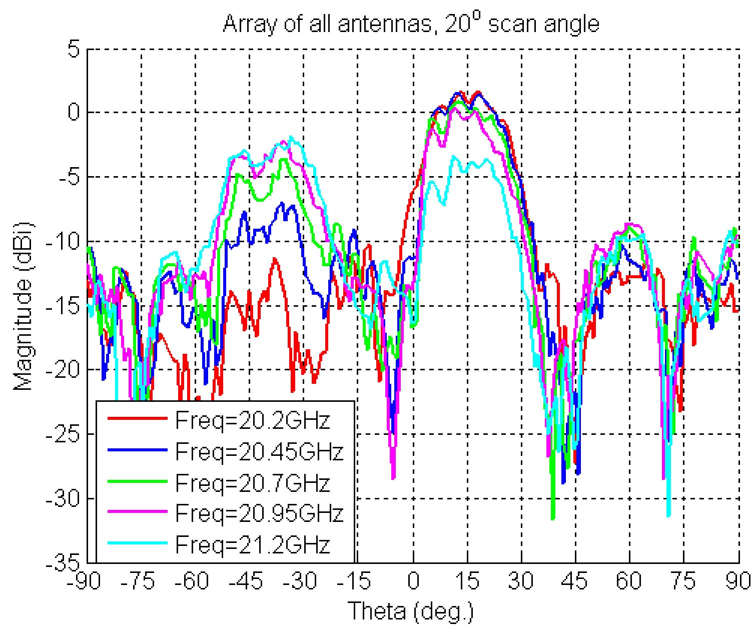

Figure 24. *Measured radiation pattern of the five-element array for a 20° scan angle at various frequencies*

The measurement of radiation patterns for 25 ° and 30 ° scan angles are also reported for several frequencies in *Figure 25* and *Figure 26*, respectively. Their characteristics are summarized in *Table 9* and *Table 10*. The behaviour is similar to the radiation patterns for a 20 ° scan angle. The beam squint is about -2 ° for a 25 ° scan angle, and -5 ° for a 30 ° scan angle. These results are similar to those obtained by simulation (see *Table 3* page 17).

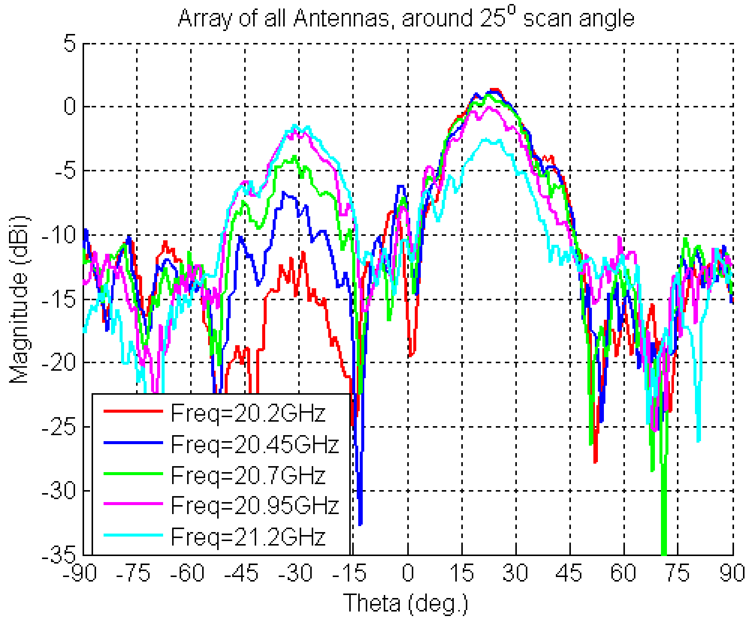

Figure 25. *Measured radiation pattern of the five-element array for a 25^{o} scan angle at various frequencies*

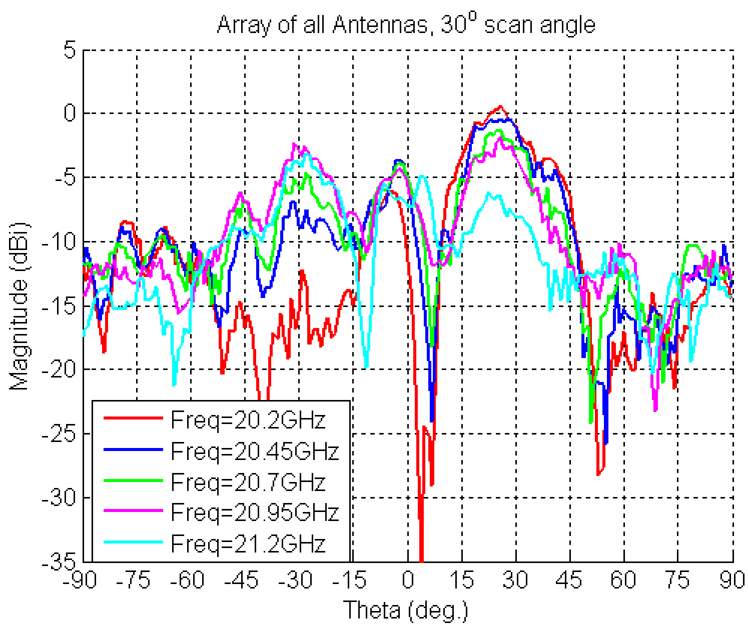

Figure 26. *Measured radiation pattern of the five-element array for a 30^{o} scan angle at various frequencies*

Table 8. *Measured radiation characteristics of the five-element array for a 20° scan angle*

Freq. (GHz)	Gain (dBi)	HPBW (deg.)	SLL (dB)
20.2	7.4	22	-11.8
20.45	7.3	21	-8.5
20.7	6.6	21	-4.4
20.95	6.2	18	-2.6
21.2	2.4	16	+1.5

Note: an adjustment of 5.8 dB corresponding to the insertion loss introduced by the feed system was made

Table 9. *Measured radiation characteristics of the five-element array for a 25° scan angle*

Freq. (GHz)	Gain (dBi)	HPBW (deg.)	SLL (dB)
20.2	7.1	20	-9.5
20.45	6.9	20	-7.4
20.7	6.6	20	-8.0
20.95	5.75	20	-7.8
21.2	3.2	19	+1.2

Note: an adjustment of 5.75 dB corresponding to the insertion loss introduced by the feed system was made

Table 10. *Measured radiation characteristics of the five-element array for a 30° scan angle*

Freq. (GHz)	Gain (dBi)	HPBW (deg.)	SLL (dB)
20.2	6.5	17	-6.8
20.45	5.5	17	-3.2
20.7	4.7	16	-2.6
20.95	4.1	16	-0.5

Note: an adjustment of 5.9 dB corresponding to the insertion loss introduced by the feed system was made

4. Conclusion and discussions

A five-element array has been investigated. This array is suitable for brick architecture array configurations. The radiating elements are rectangular waveguides realised in laminated technology. The fabrication process is compatible with LTCC technology. In this design the vertical walls are created with vias. The impedance bandwidth of the coaxial-to-waveguide transition is very wide (17 GHz to more than 25 GHz), but the aperture matching circuit narrows down the impedance bandwidth of the radiating element to 1 GHz. The radiation patterns of the laminated waveguide are similar to those of a conventional rectangular waveguide, and the measured gain of the radiating element is 2.7 dBi.

In array configuration the element impedance bandwidth is slightly shifted up in frequency due to the mutual coupling, which however remains below –20 dB in the worst case. The radiation patterns of the array are stable across the operating bandwidth (20.2 GHz to 21.2 GHz) and the gain is 9.2 dBi at the centre frequency. The measurements confirmed the results obtained by simulation. This array shows also a good scanning behaviour up to 50^{o}. Measurements of radiation patterns for several scan angles have demonstrated the scanning capability of this array.

The results obtained with our prototypes point out some issues regarding the effects of fabrication tolerances. These issues will be considerably reduced if the elements were realised with LTCC process. In fact, to our knowledge, fabrication tolerances are more controlled with the LTCC process than with our PCB fabrication process. For the probe and capacitive posts for instance, their length will be precisely a multiple of layer thickness, and will therefore not depend on the drilling depth accuracy. The frequency shift of the impedance responses will then be considerably reduced.

Laminated waveguides are suitable for applications when the total substrate thickness is large compared to the wavelength. This design can be scaled for higher frequency applications, or when a material of higher permittivity is used. The main constraint remains the via diameter and pitch. For an LTCC process, the minimum via diameter and pitch vary from one foundry to another, but the via diameter is about 100-150µm and the via pitch is about 2.5 times the via diameter.

Our five-element array prototype shows that the laminated radiating waveguide can be used in a phased array. Phase shifters can be used to steer the beam but the difference of propagation constant dispersion in the short and long LWGs and in the phase shifters is an issue for measurement at various frequencies. A further study could consider elements of the same length to better control the phase distribution across the array.

The work reported here concentrates on a radiating element in laminated technology to be used in array configuration for scanning applications. For this reason, an open waveguide was chosen rather than a horn to obtain a large beamwidth, and therefore a low gain. A study focusing on high-gain element using laminated technology will be complementary to this first investigation on radiating laminated waveguides.

5. References

[1] Litzenberger, J.O., Clénet, M., Morin G. A., Antar, Y. M. M., (2002) "Study of a *Waveguide Antenna Implemented in Laminated Material*", DRDC Ottawa TR 2002-132, Defence R&D Canada - Ottawa.

[2] J. Hirokawa, M. Ando, "*Single-layer Feed Waveguide Consisting of Posts for Plane TEM Wave Excitation in Parallel Plates*", IEEE Trans. on Antennas and Propagation, May 1998,vol. 46, no. 5, pp. 625-630

[3] H. Uchimura, T. Takenoshita, and M. Fujii, "*Development of a Laminated Waveguide*", IEEE Trans. on Microwave Theory and Techniques, December 1998,vol. 46, no. 12, pp. 2438-2443.

[4] J. Bray, and L. Roy, "*Laminated Waveguide Couplers in LTCC Technology*", ANTEM 2000 August 2000, pp. 527-530.

[5] Uchimura, H., Takenoshita, T "*A Ceramic Planar 77GHz Antenna Array*", Microwave Symposium Digest, 1999 IEEE MTT-S International , Vol 2 , 1999, pp. 453 –456.

[6] J. Litzenberger, M. Clénet, G. A. Morin and Y. M. M. Antar, "*A New Antenna Implemented in Laminated Waveguide*", ANTEM 2002, 31 July – 2 August, 2002, Montréal, Québec.

[7] B. Geller, B. Thaller, A. Fathy, M. J. Liberatore, H. D. Chen, G. Ayers, V. Pendrick and Y. Narayan, "*LTCC-M: an Enabling Technology for High Performance Multilayer RF Systems*", Microwave Journal, Vol. 42, No. 7, July 1999, pp 64-72.

[8] D. Sturzebecher, J. Leen, R. Cadotte, J. DeMarco, T-D. Ni, T. Higgins, M. Popick, M. Cummings, B. VanMeerbeke, T. Provencher, B. Kimble, K. Shalkhauser, R. Simons, "*20 GHz LTCC Phased Array Module*", IEEE MTT International Symposium, 1996, Vol. 2, pp 991-994.

[9] DuPont Microcircuit Materials, "*Characterization of Low Loss LTCC Materials at 40GHz*", Microwave Journal, Vol. 44, No 2, February 2001, pp 186-190.

[10] Desclos, L., "*V-Band Double-Slot Antenna Integration on LTCC Substrate using Thin Film Technology*", MOTL, Vol. 28, No. 5, March 5 2001, pp 354-357.

[11] Lin, C.-C., Chang, Y.-J. and Chuang, H.-R., "*Design of a 900/1800 MHz Dual-Band LTCC Chip Antenna for Mobile Communications Applications*", Microwave Journal, Vol. 47, No. 1, pp 78-88.

[12] Li, R., DeJean, G., Maeng, M., Lim, K. Pinel, S. Tentzeris, M. M., Laskar, J., "*Design of Compact Stacked-Patch Antennas in LTCC Multilayer Packaging Modules for Wireless Applications*", IEEE Trans. On Advanced Packaging, Vol. 27, No. 4, Novembre 2004, pp 581-589.

[13] Clénet, M., "*Study of a Ka-Band Yagi-like antenna array buried in LTCC material*", JINA, 12-14 November 2002, Nice, France, Vol.2, pp 165-168.

[14] High Frequency Structure Simulator, www.ansoft.com

[15] Sherman, J., "Application Note: Introduction to Impedance Definitions", ANSOFT: September 9, 1998. pp 1-14.

Annexes

Annex 1. Characteristiscs of arrays of five short and five long radiating LWGs

Array of five short radiating laminated waveguides simulated with a 3” by 2” substrate. Array of five long radiating LWGs simulated with a 3” by 3” substrate.

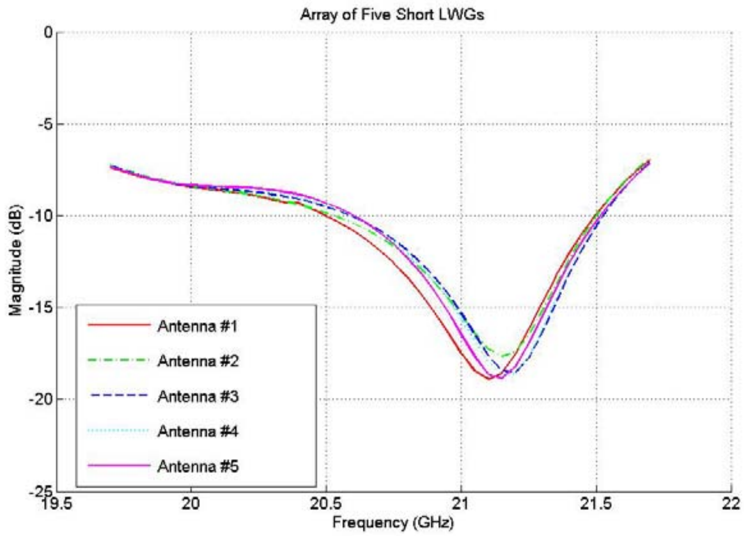

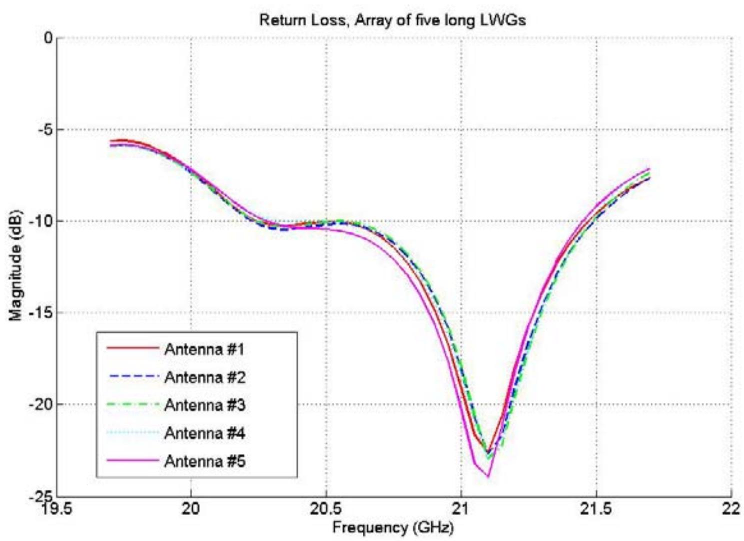

Figure 27. *Return loss for the radiating elements of the arrays of five short and five long radiating LWGs*

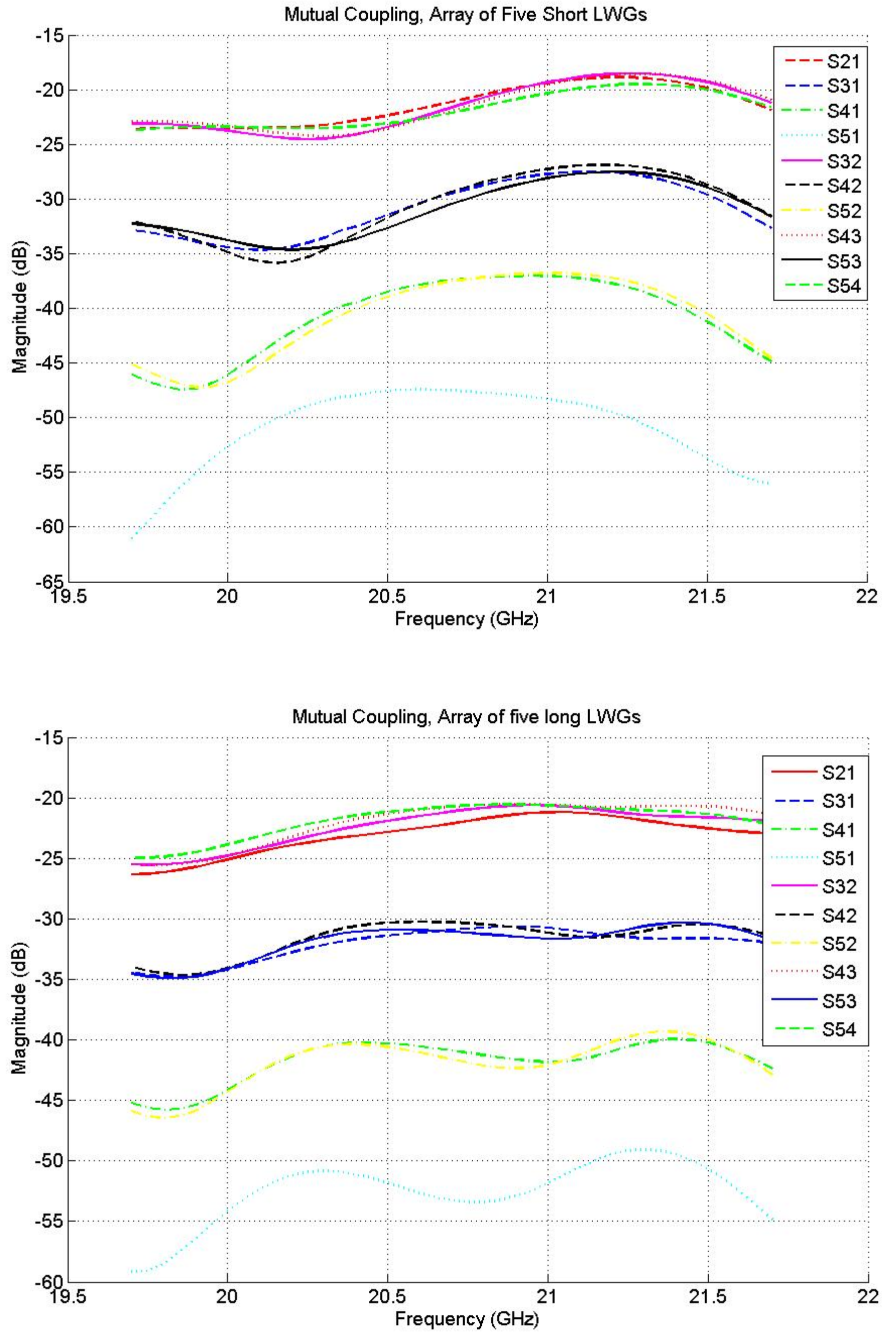

Figure 28. *Mutual coupling for the arrays of five short and five long radiating LWGs*

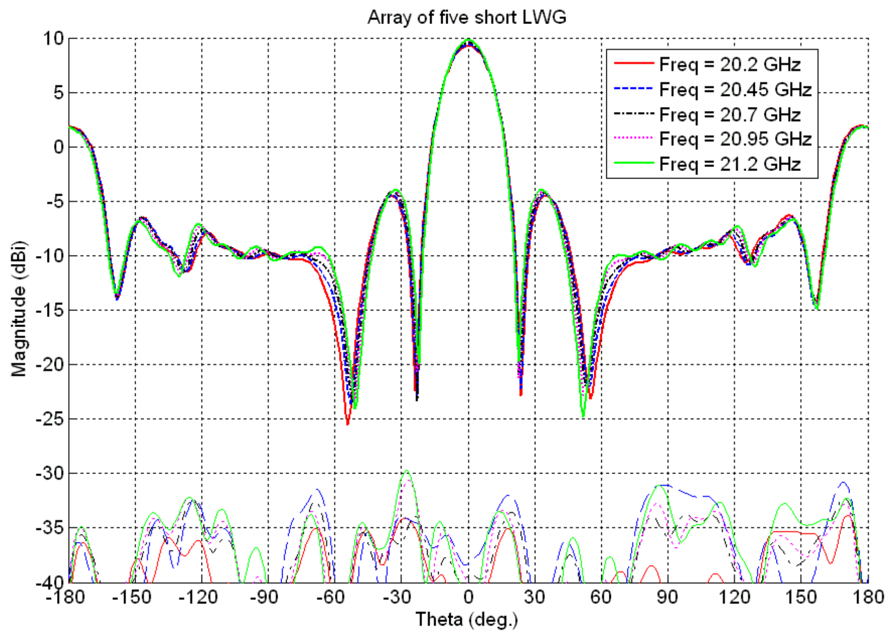

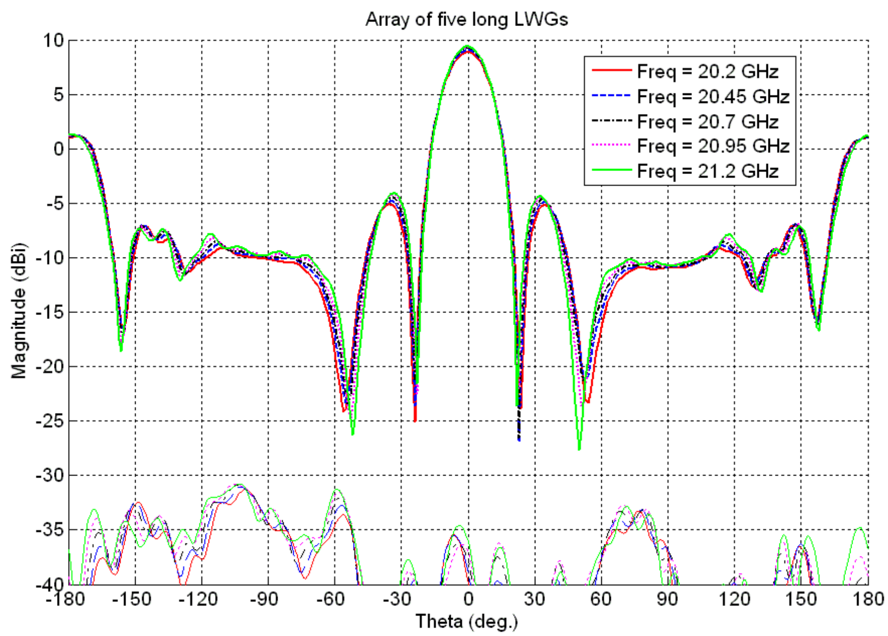

Figure 29. *Boresight radiation patterns for the radiating elements of the arrays of five short and five long radiating LWGs*

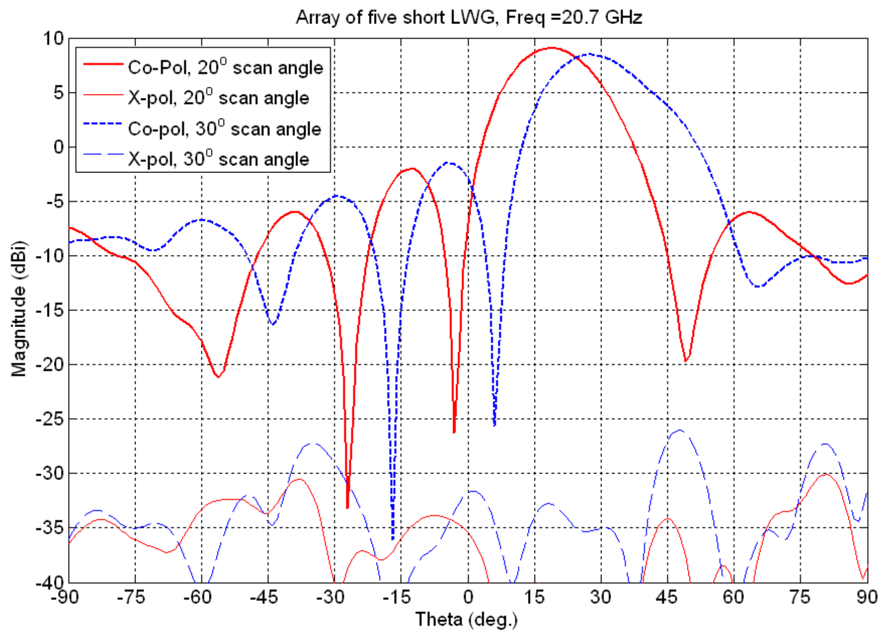

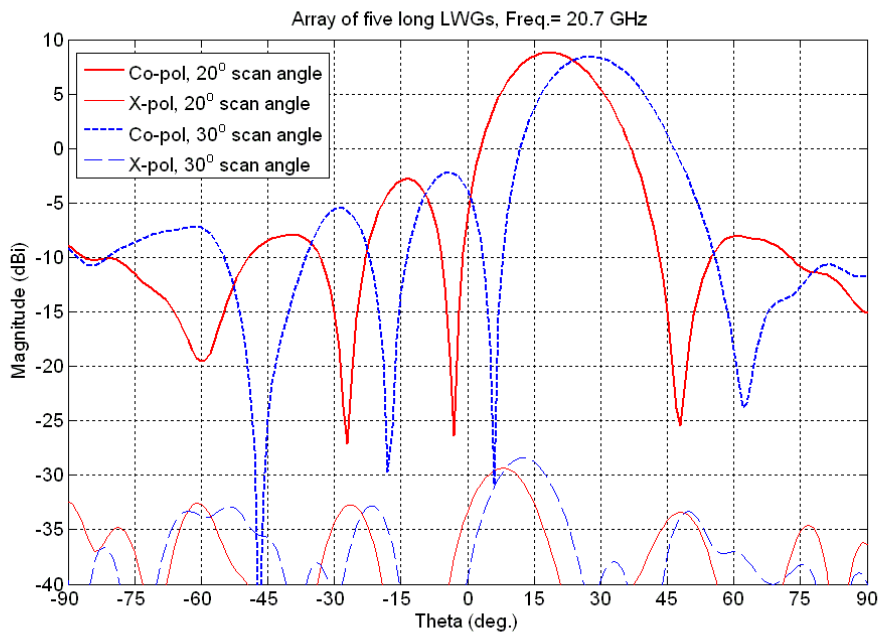

Figure 30. *Radiation patterns for 20^o and 30^o scan angles for the radiating elements of the arrays of five short and five long radiating LWGs at 20.7 GHz*

Table 11. *Characteristics of simulated radiation patterns in the boresight direction for an array of the five short radiating LWGs*

Freq. (GHz)	Gain (dBi)	HPBW (deg.)	SLL (dB)
20.2	9.3	22	-13.75
20.45	9.4	22	-13.8
20.7	9.6	21	-13.7
20.95	9.7	21	-13.8
21.2	9.8	20	-13.7

Note: The radiation patterns were simulated every degree

Table 12. *Characteristics of simulated radiation patterns in the boresight direction for an array of the five long radiating LWGs*

Freq. (GHz)	Gain (dBi)	HPBW (deg.)	SLL (dB)
20.2	8.8	22	-13.9
20.45	9.1	21	-13.85
20.7	9.2	21	-13.7
20.95	9.3	21	-13.5
21.2	9.4	21	-13.4

Note: The radiation patterns were simulated every degree

Table 13. *Characteristics of simulated radiation patterns for 20^o and 30^o scan angle for an array of the five short radiating LWGs at 20.7 GHz*

Scan angle (deg.)	Angle at max. gain (deg.)	Gain (dBi)	HPBW (deg.)	SLL (dB)
20	19	9.0	22	-11.1
30	28	8.4	24	-9.92

Note: The radiation patterns are evaluated every degree

Table 14. *Characteristics of simulated radiation patterns for 20^o and 30^o scan angle for an array of the five long radiating LWGs at 20.7 GHz*

Scan angle (deg.)	Angle at max. gain (deg.)	Gain (dBi)	HPBW (deg.)	SLL (dB)
20	19	8.8	22	-11.6
30	28	8.4	23	-10.6

Note: The radiation patterns are evaluated every degree

Annex 2. Power divider characteristics

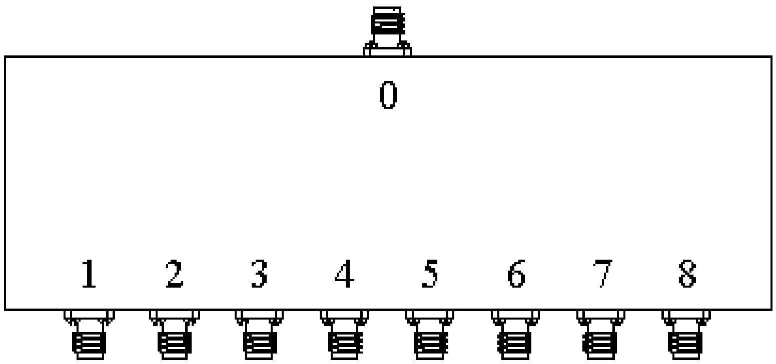

Figure 31. *Sketch of the 8-way power divider*

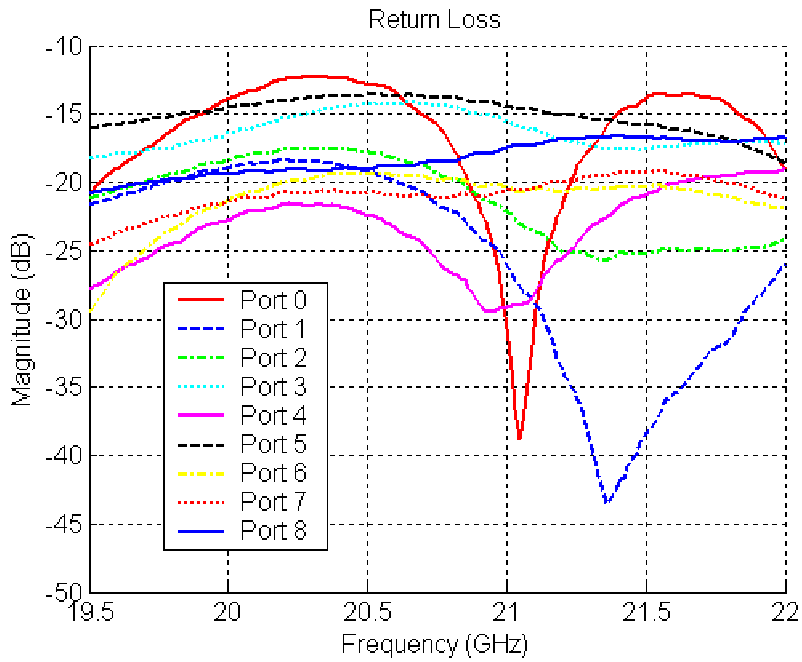

Figure 32. *Return loss for the input and outputs of the 8-way power divider*

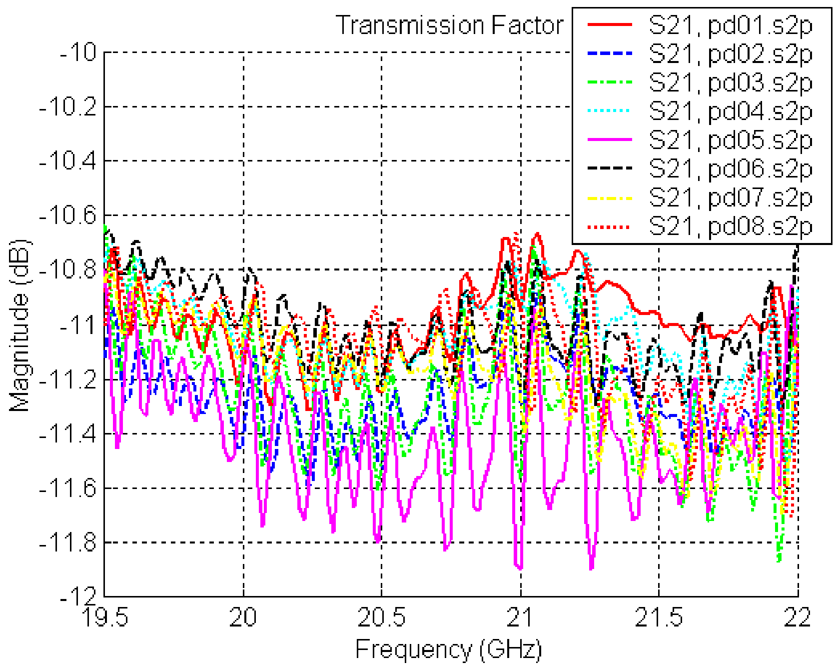

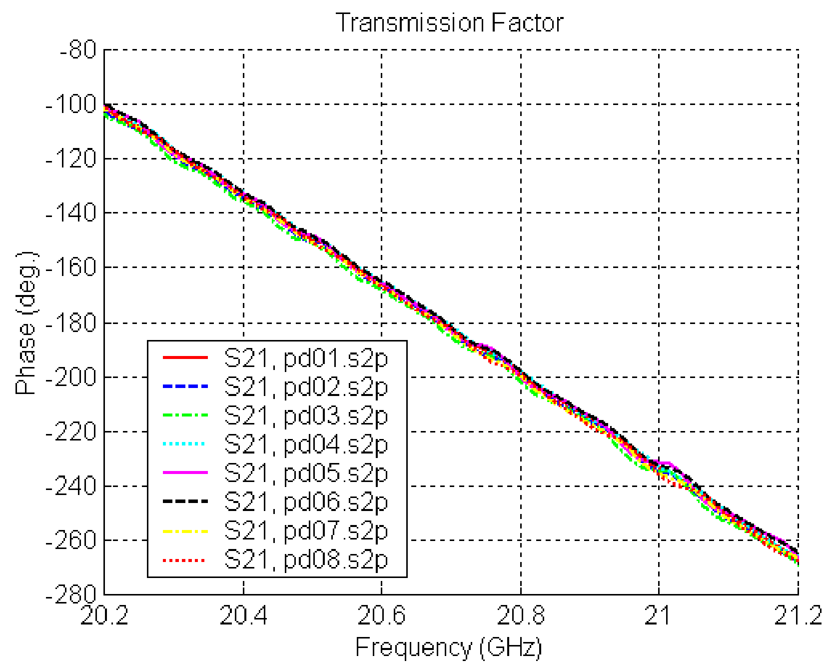

Figure 33. *Transmission factor for the 8-way power divider*

a) Coupling for output #1

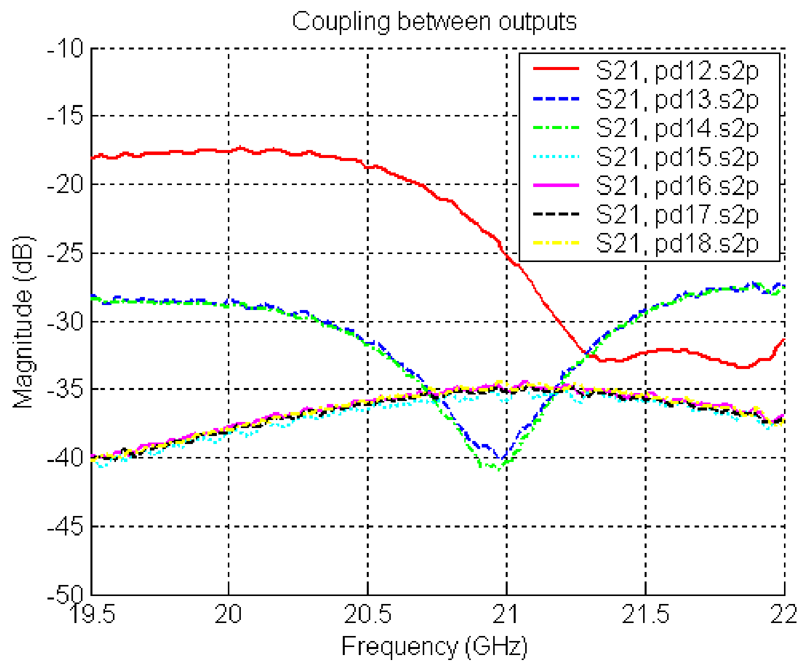

b) Coupling for output #2

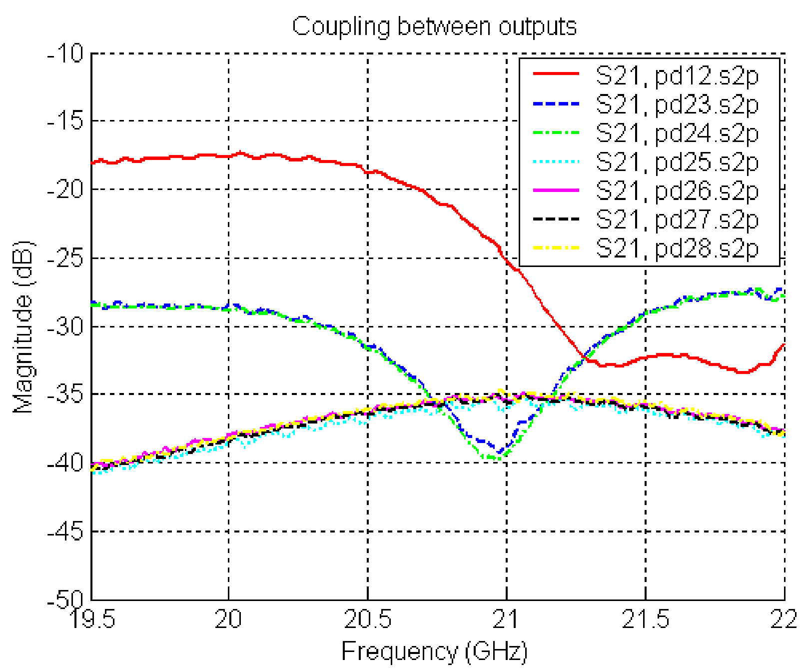

c) Coupling for output #3

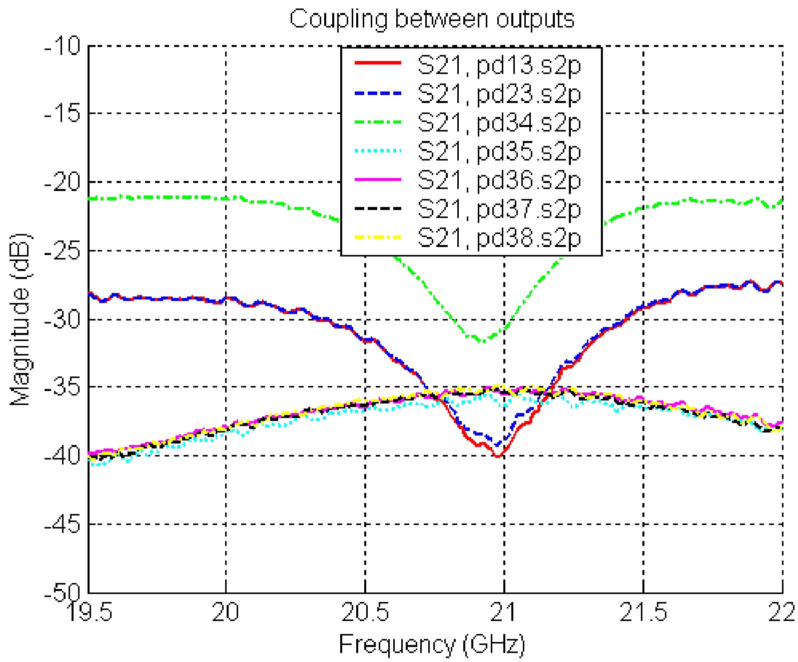

d) Coupling for output #4

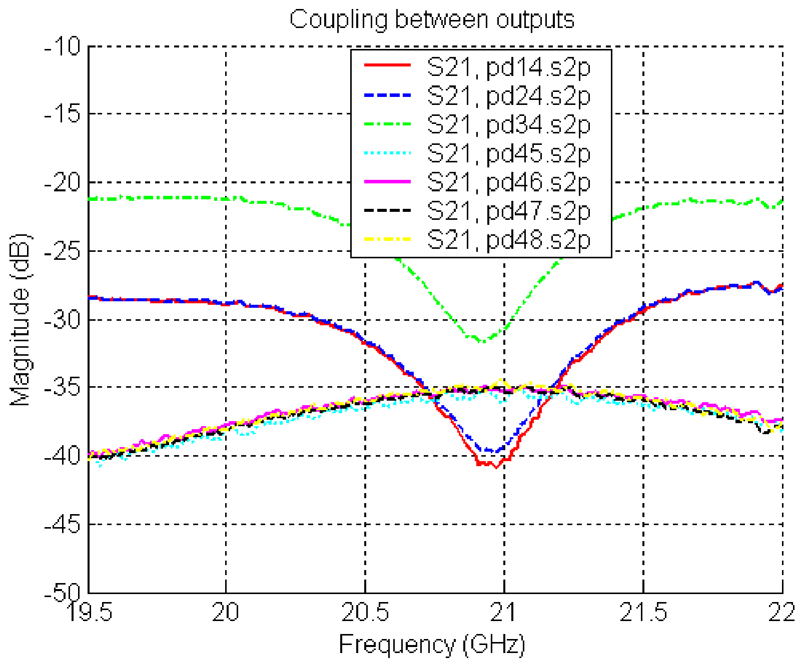

e) Coupling for output #5

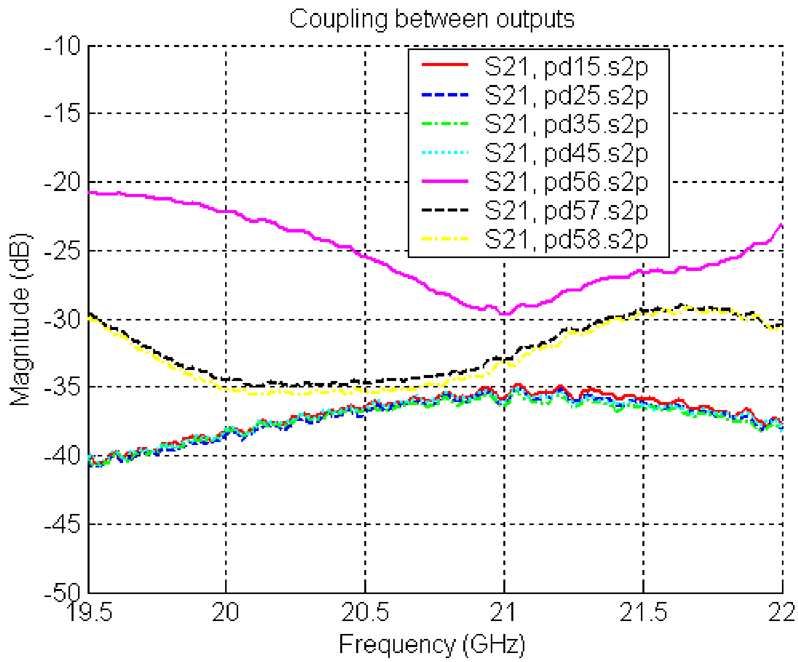

f) Coupling for output #6

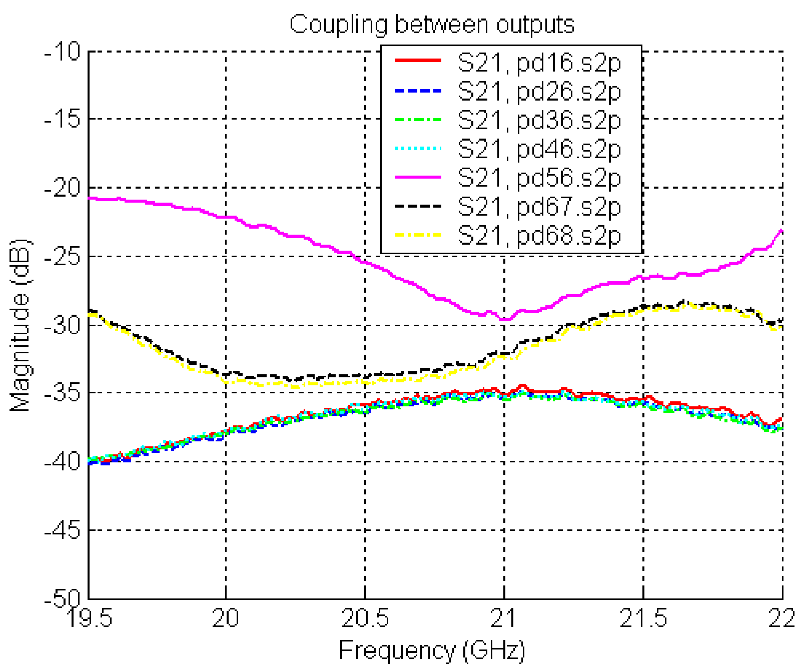

g) Coupling for output #7

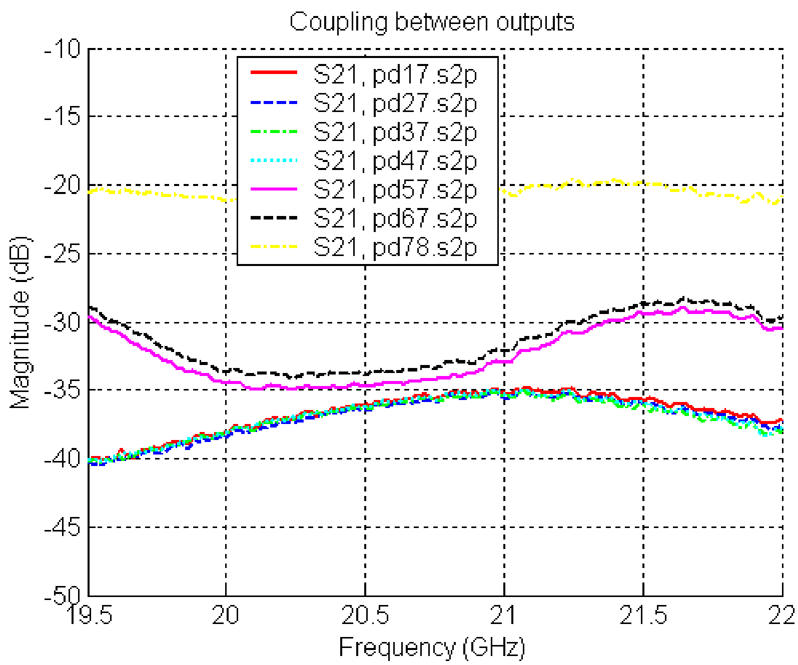

h) Coupling for output #8

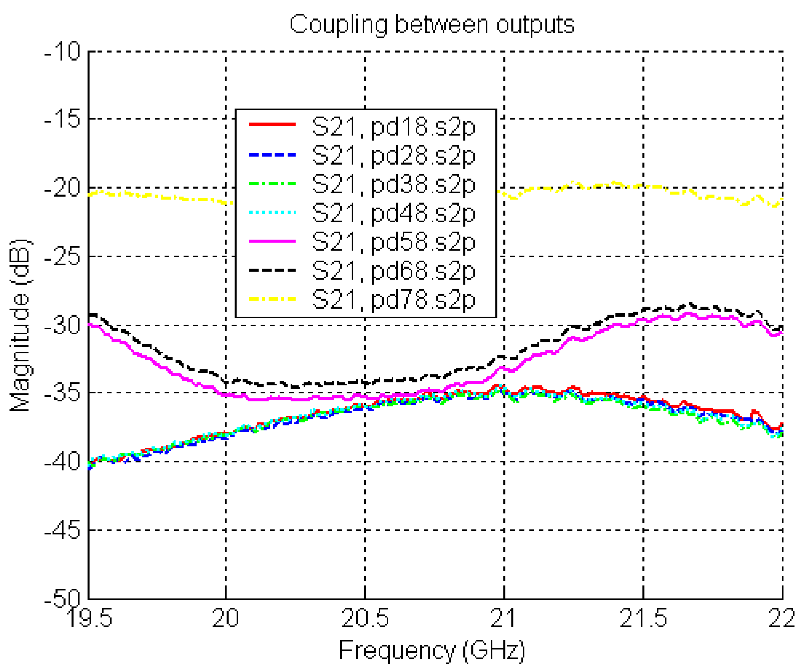

Figure 34. *Mutual coupling between power divider outputs*

Annex 3. Line stretcher characteristics

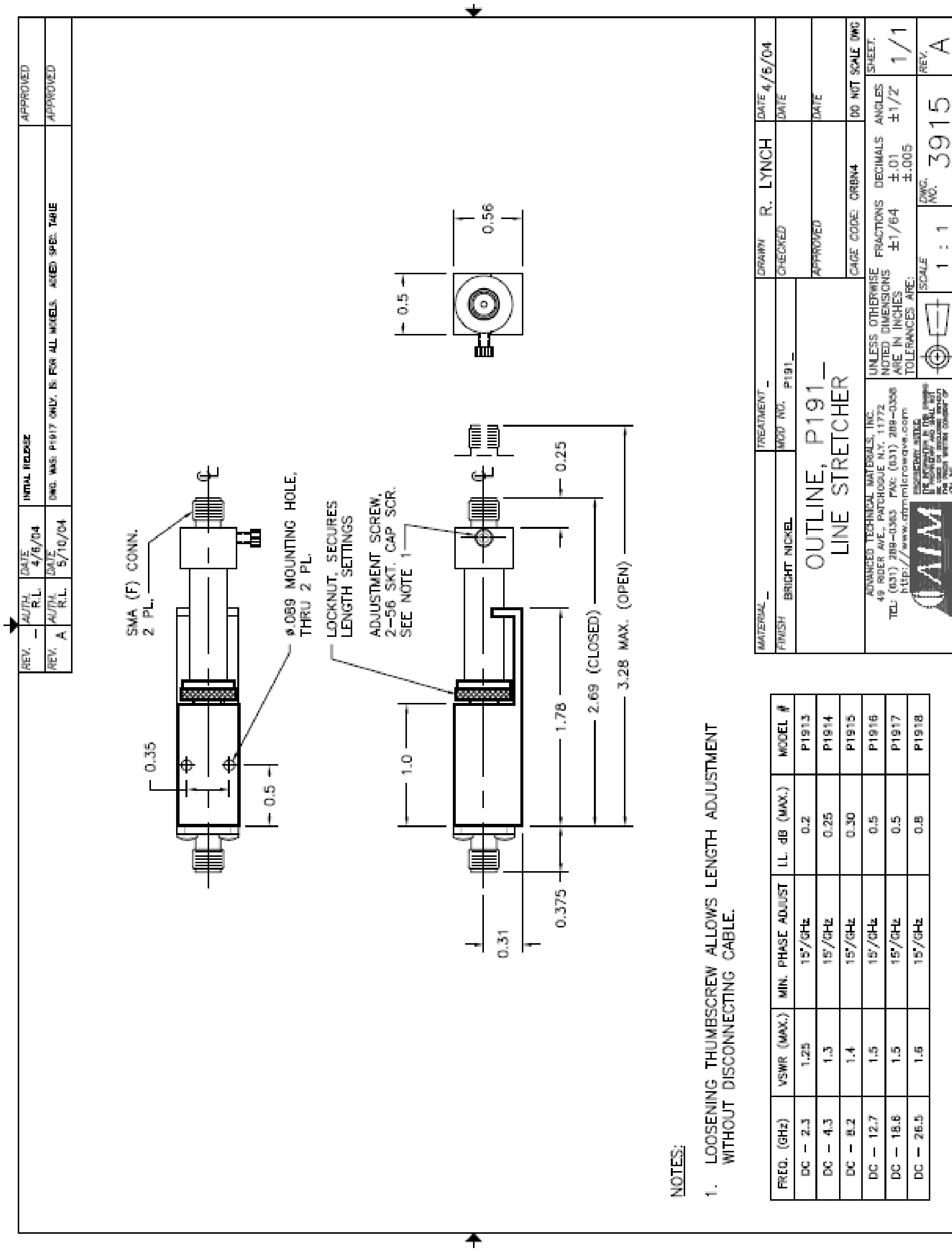

Figure 35. *Drawing of the line stretcher*

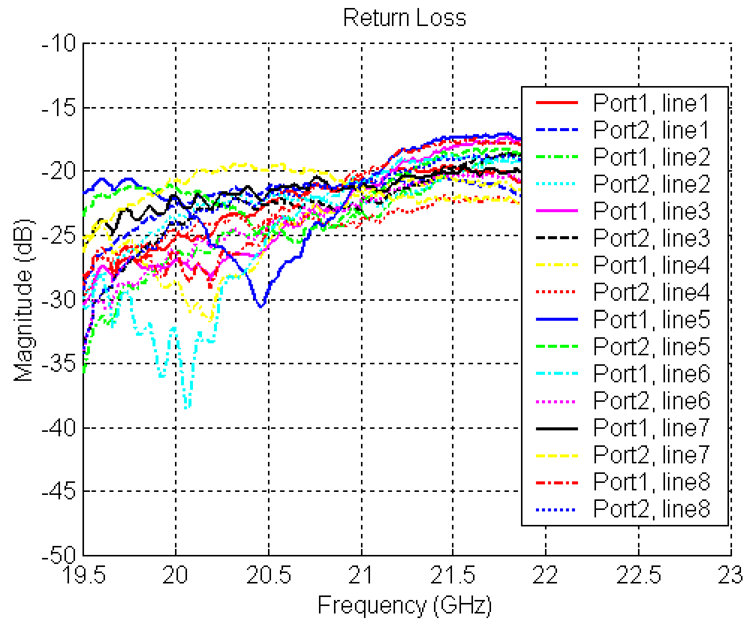

Figure 36. *Return loss of the line stretchers in the 'short' position*

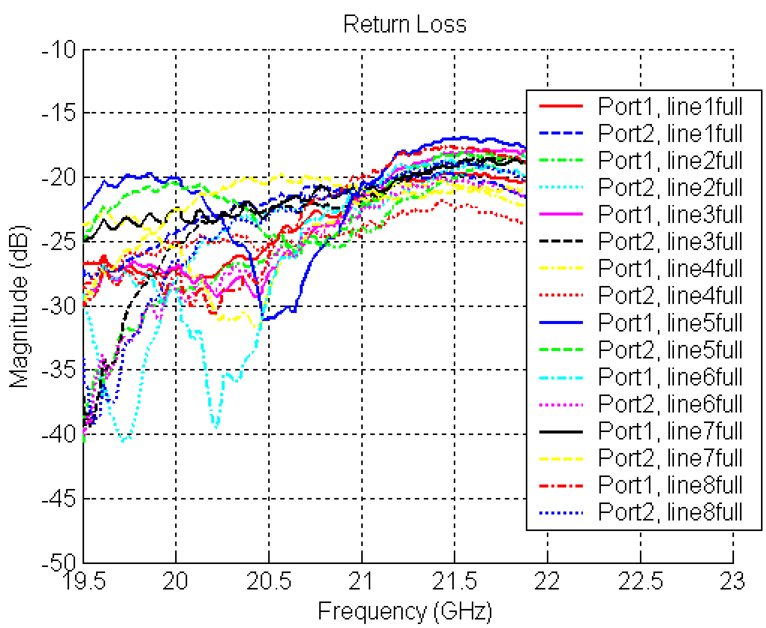

Figure 37. *Return loss of the line stretchers in the 'long' position*

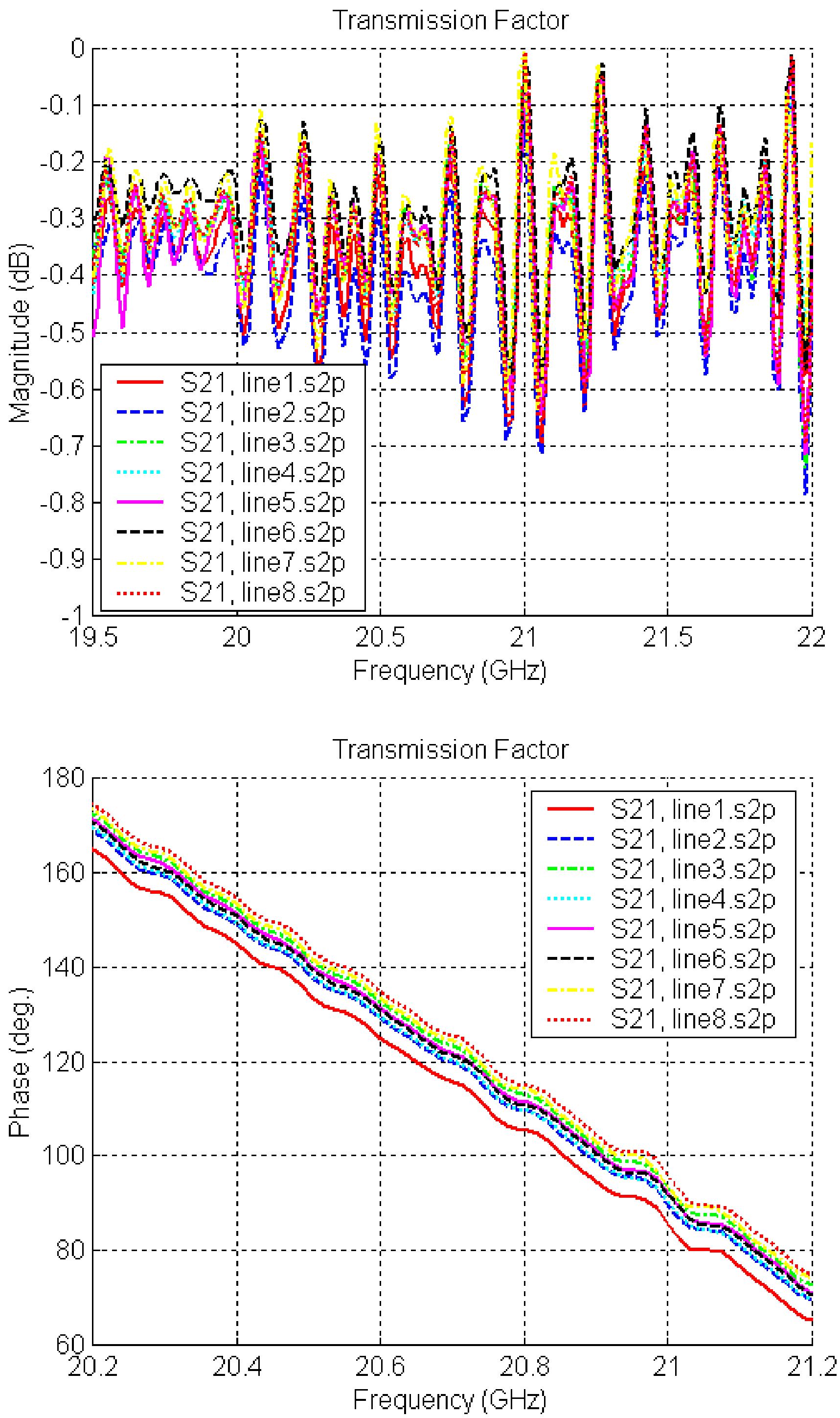

Figure 38. *Transmission factor of the line stretchers in the 'short' position*

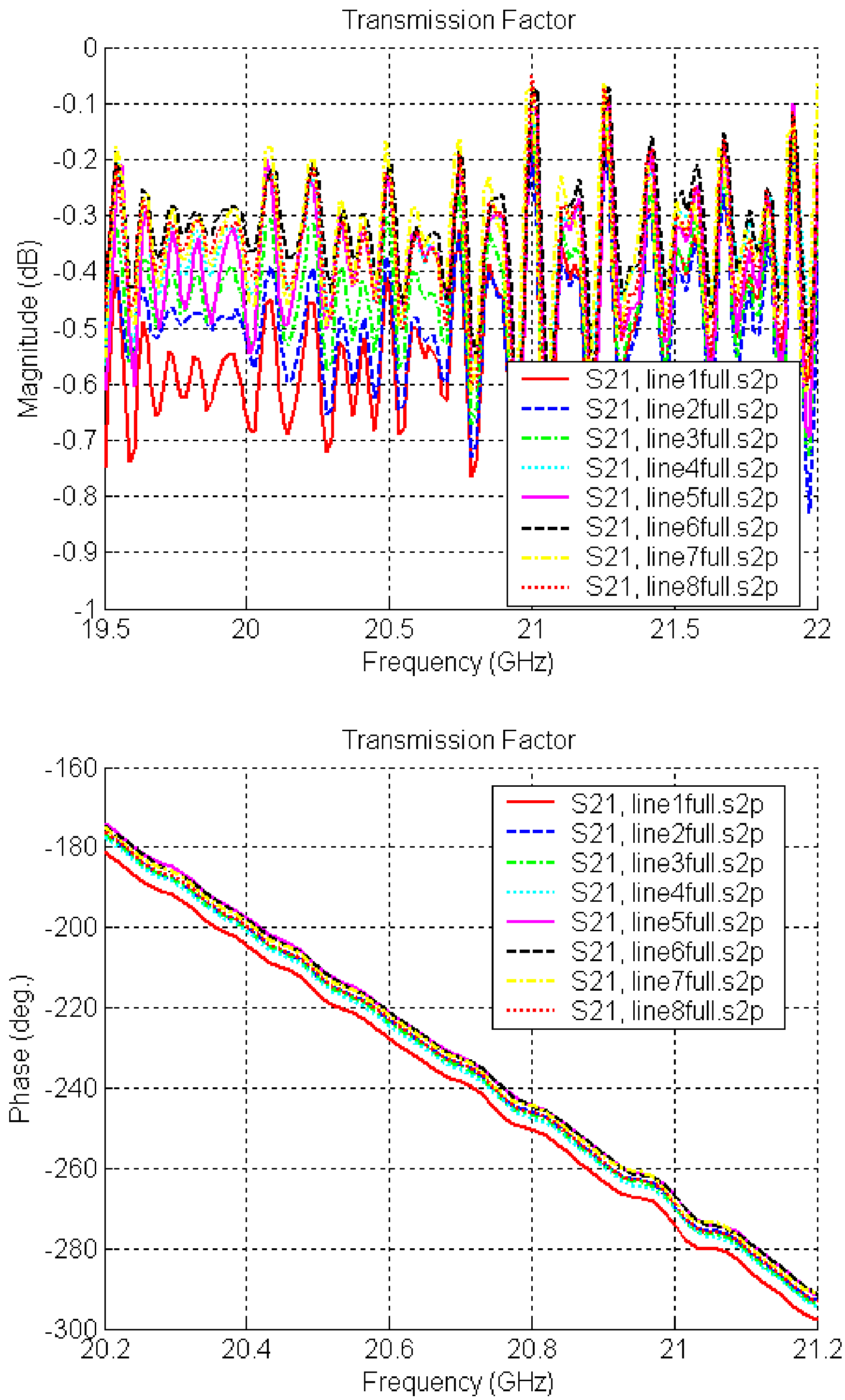

Figure 39. *Transmission factor of the line stretchers in the 'long' position*

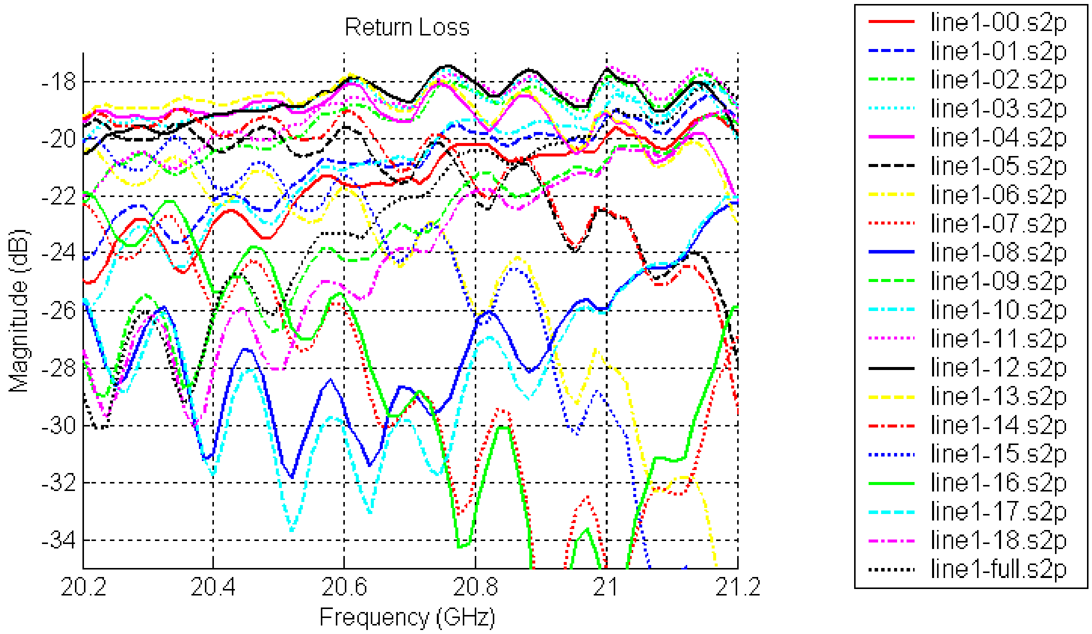

Figure 40. *Return loss of line stretcher #1 for several positions*

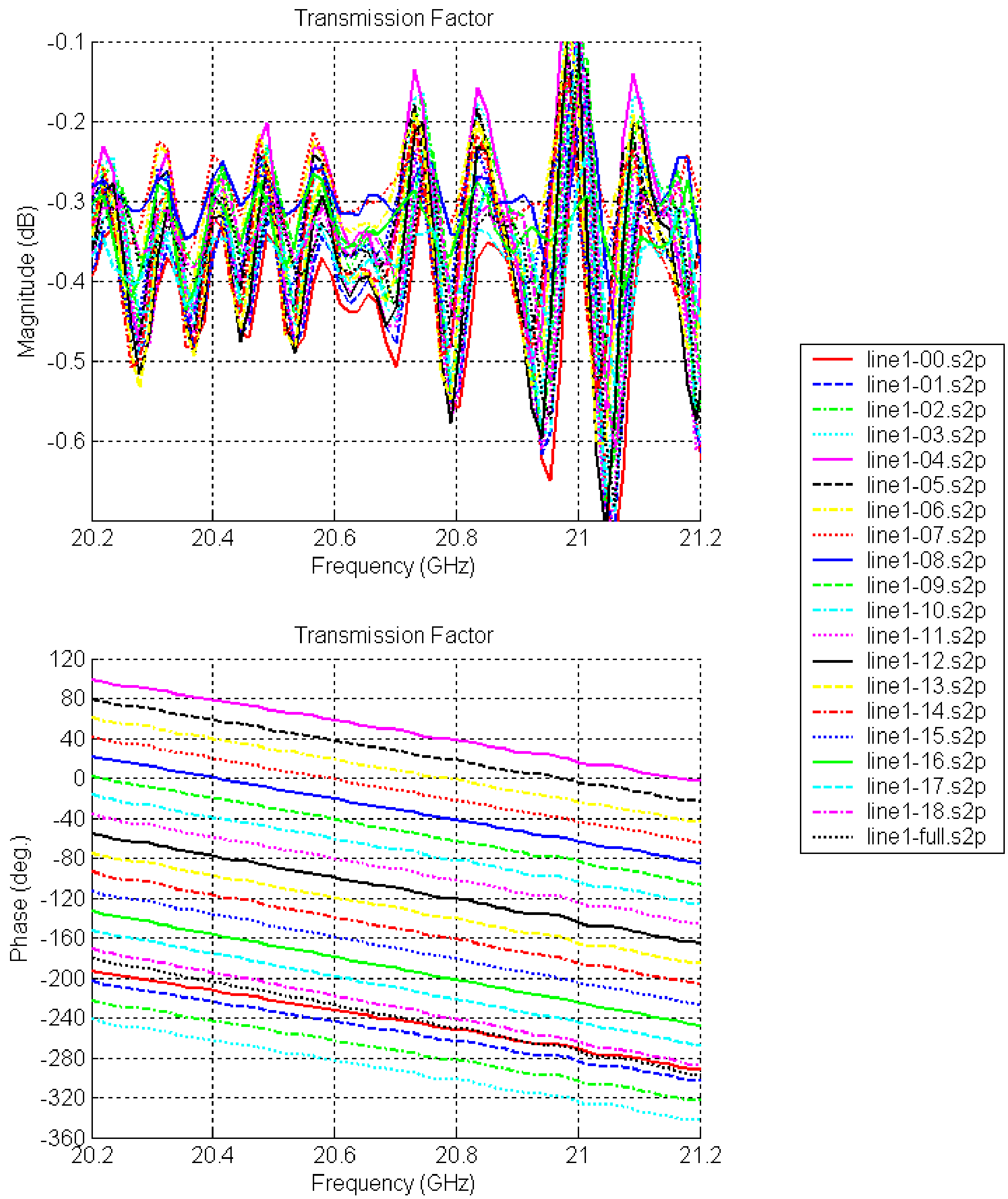

Figure 41. *Transmission factor of line stretcher #1 for several positions*

Annex 4. Constant-phase cable characteristics

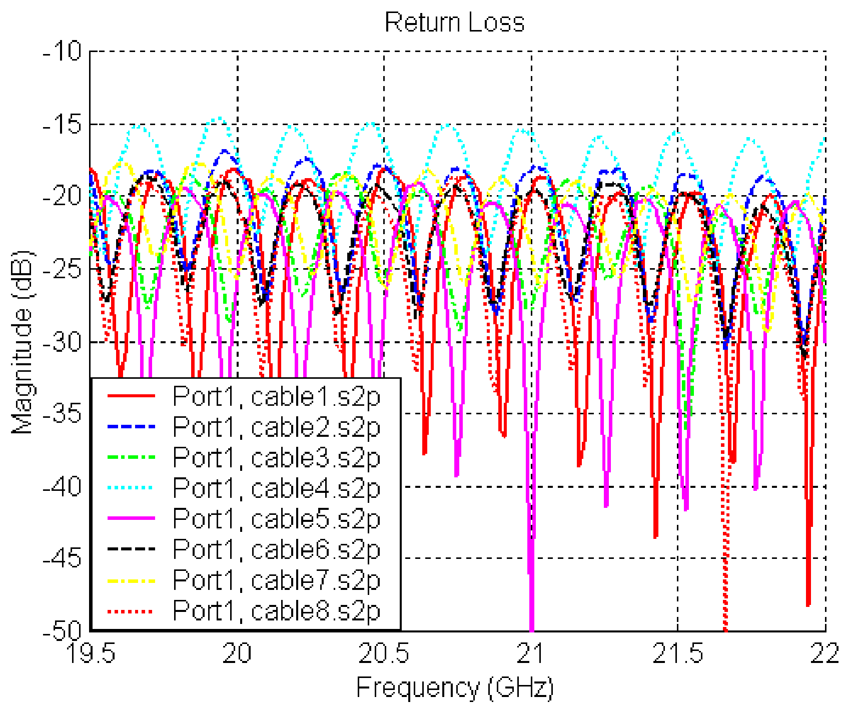

Figure 42. *Return Loss of the constant phase cables*

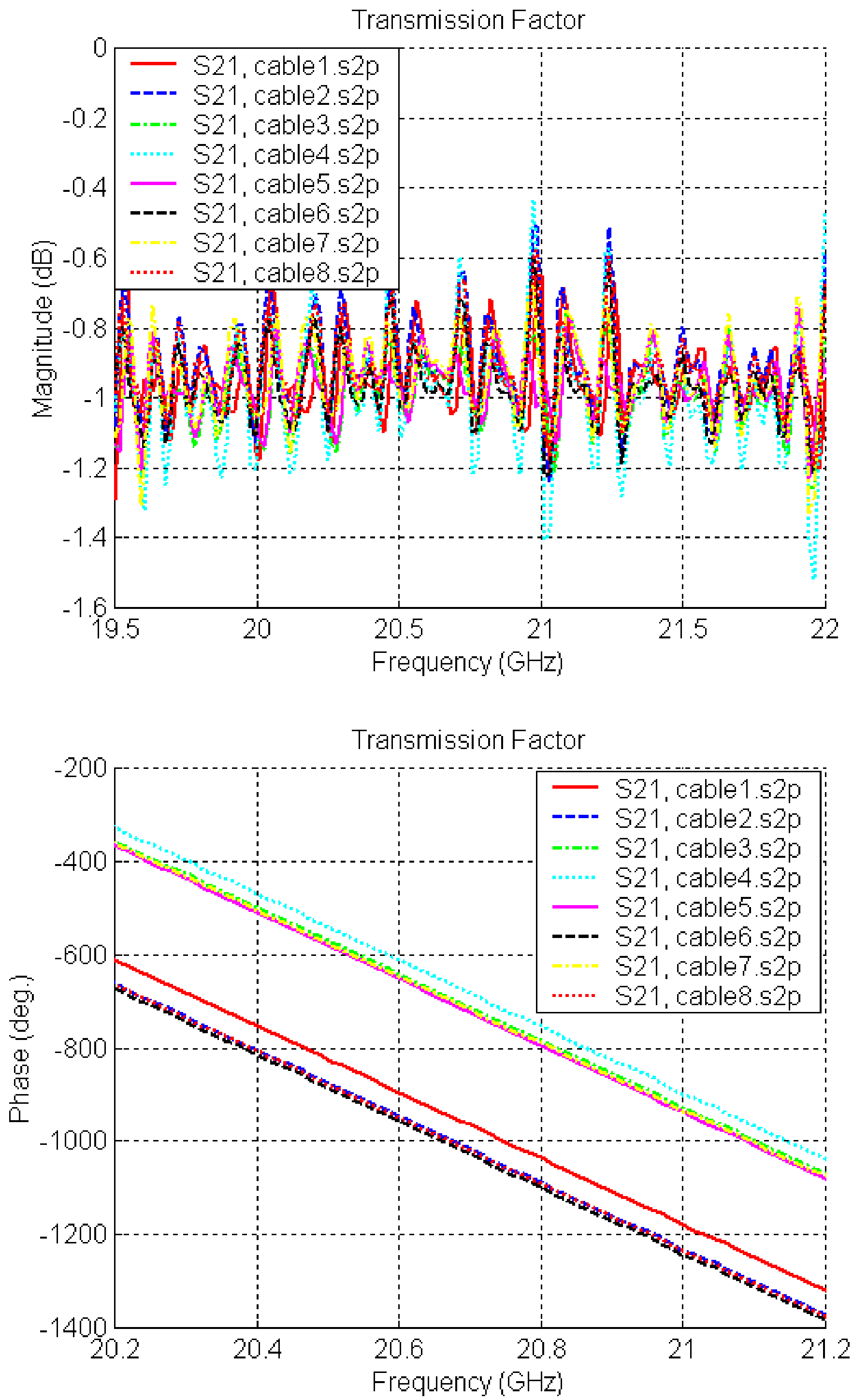

Figure 43. *Transmission factor of the constant-phase cables*

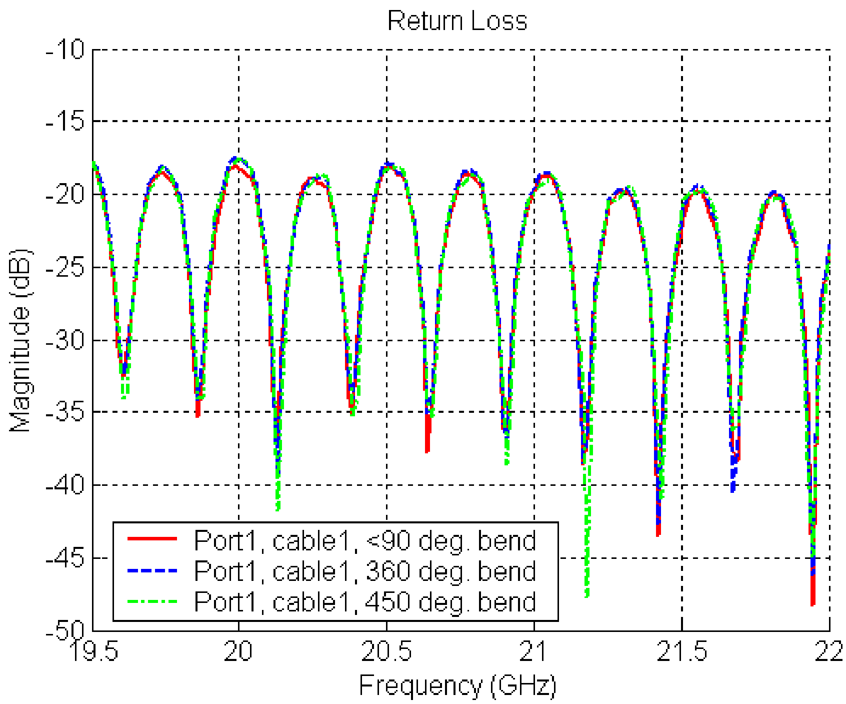

Figure 44. *Return loss of cable #1 for several bent angles*

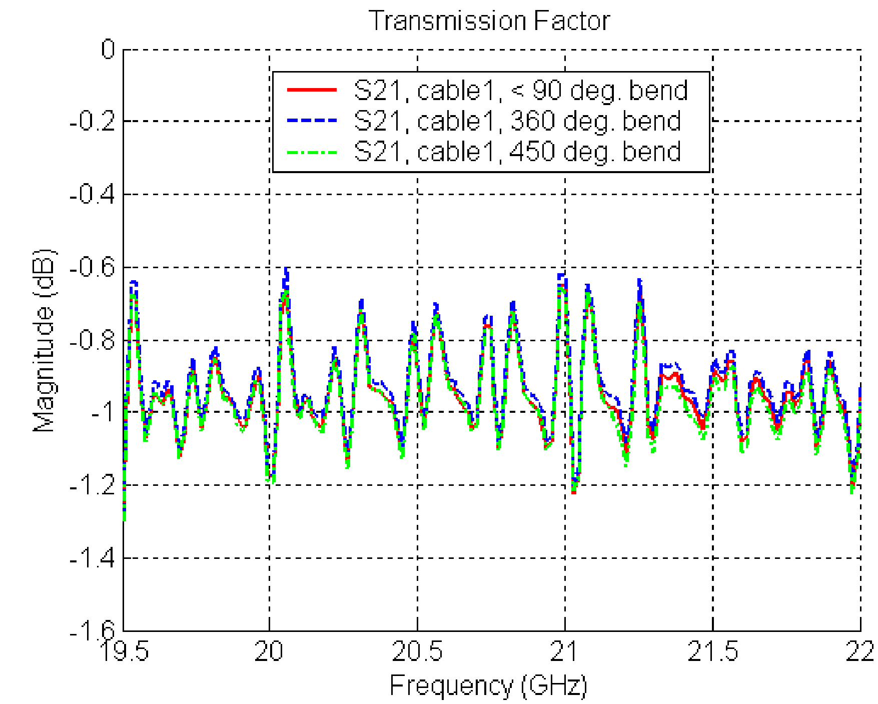

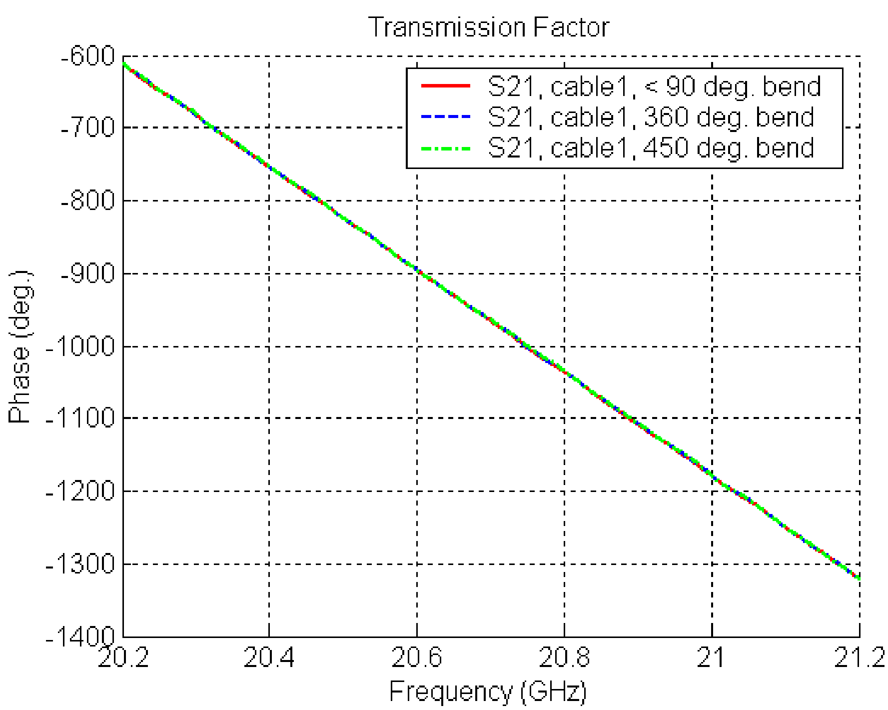

Figure 45. *Transmission factor of cable #1 for several bent angle*

Annex 5. Swept ninety-degree bend characteristics

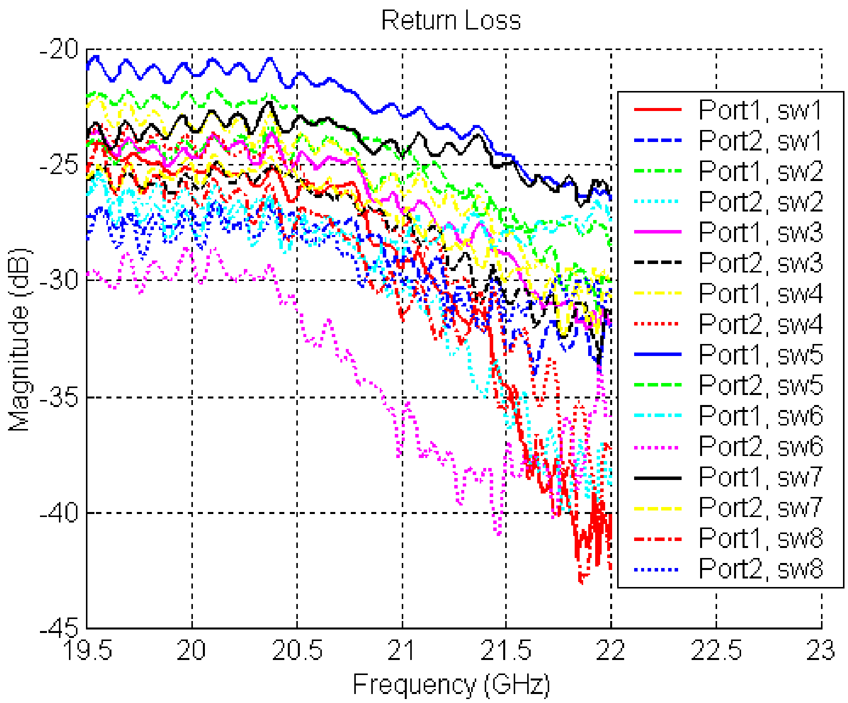

Figure 46. *Reflection coefficient of the swept ninety-degree bends*

Table 15. *Transmission factor at 20.7 GHz of the 90^o bends*

Bend #	1	2	3	4	5	6	7	8
Magnitude (dB)	-0.28	-0.21	-0.26	-0.2	-0.25	-0.26	-0.175	-0.2
Phase (deg.)	113	116	118	118	122	114	116	114

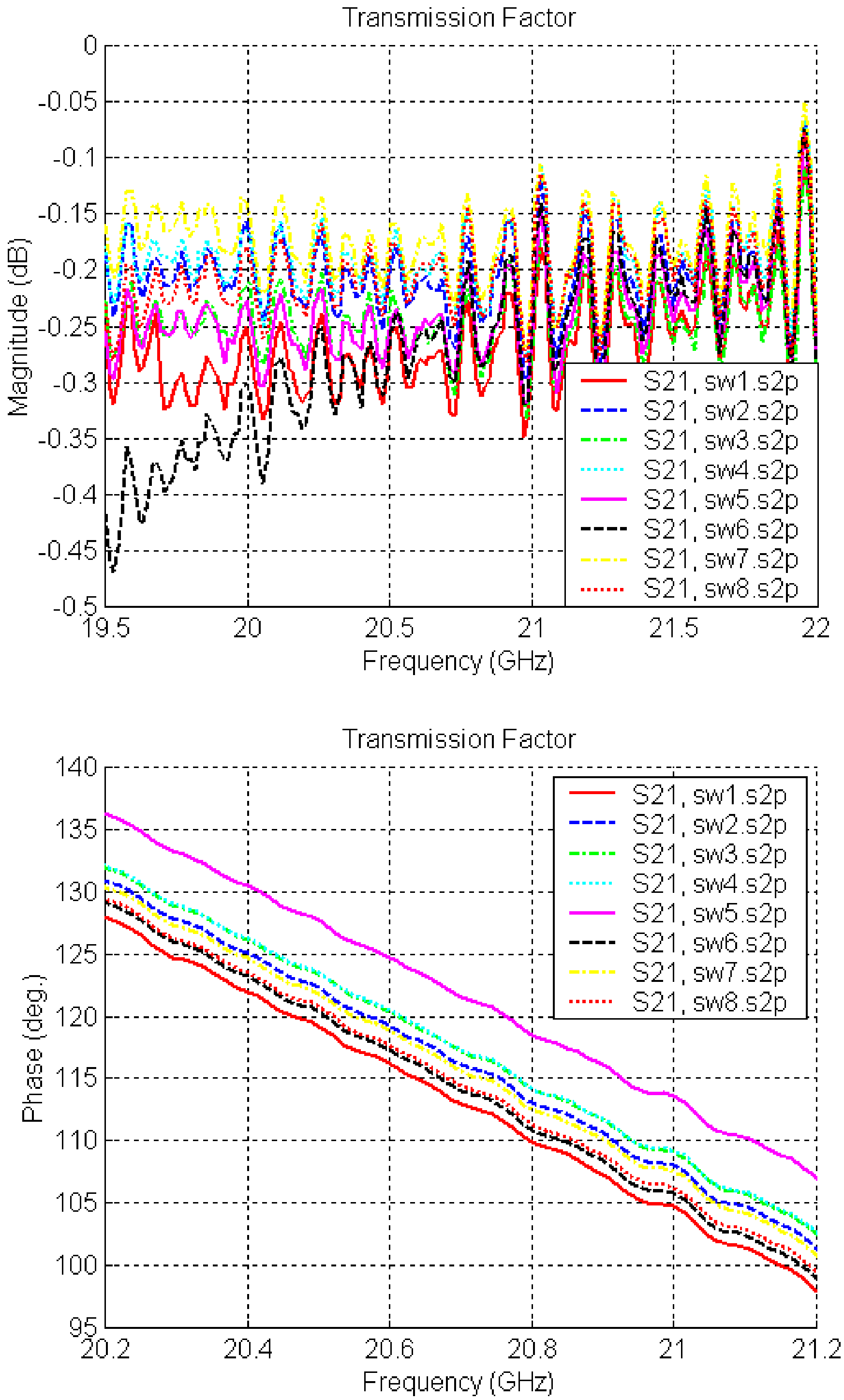

Figure 47. *Transmission factor of the swept ninety-degree bends*

List of symbols/abbreviations/acronyms/initialisms

CLTE	Controlled Low Thermal Expansion
DND	Department of National Defence
HFSS	High Frequency Structure Simulator
HPBW	Half-Power Beam Width
IL	Insertion Loss
LTCC	Low Temperature Co-fired Ceramic
LWG	Laminated Waveguide
MIC	Microwave Integrated Circuit
PCB	Printed Circuit Board
RL	Return Loss
RWG	Rectangular Waveguide
SHF	Super High Frequency
SLL	Side Lobe Level
VNA	Vector Network Analyser

Distribution list

External

- DRDKIM 1
- Library and Archive Canada 2
- CISTI 1
- David Lee 1

  CRC

  Antenna Test Facility (ATF), Blg 2C, room 152A

  3701 Carling Avenue

  Ottawa, Ont., Canada
- Yahia Antar 1

  Dept. of Electrical and Computer Engineering

  Royal military College of Canada

  Kingston, Ontario K7K 5L0, Canada

Internal

- CNEW/SH 1
- CNEW/Navigation/GL 1
- Library 3
- Author (M. Clénet) 2

Total 13

DOCUMENT CONTROL DATA

(Security classification of title, body of abstract and indexing annotation must be entered when the overall document is classified)

1. ORIGINATOR (the name and address of the organization preparing the document. Organizations for whom the document was prepared, e.g. Establishment sponsoring a contractor's report, or tasking agency, are entered in section 8.) Defence R&D Canada – Ottawa Ottawa, On, K1A 0Z4	2. SECURITY CLASSIFICATION (overall security classification of the document, including special warning terms if applicable) UNCLASSIFIED

3. TITLE (the complete document title as indicated on the title page. Its classification should be indicated by the appropriate abbreviation (S,C or U) in parentheses after the title.)

Array of Laminated Waveguides for Implementation in LTCC Technology (U)

4. AUTHORS (Last name, first name, middle initial)

Clénet, Michel, Lee, David and Antar, Yahia M. M.

5. DATE OF PUBLICATION (month and year of publication of document) November 2006	6a. NO. OF PAGES (total containing information. Include Annexes, Appendices, etc.) 61	6b. NO. OF REFS (total cited in document) 15

7. DESCRIPTIVE NOTES (the category of the document, e.g. technical report, technical note or memorandum. If appropriate, enter the type of report, e.g. interim, progress, summary, annual or final. Give the inclusive dates when a specific reporting period is covered.)

Technical Memorandum

8. SPONSORING ACTIVITY (the name of the department project office or laboratory sponsoring the research and development. Include the address.)

9a. PROJECT OR GRANT NO. (if appropriate, the applicable research and development project or grant number under which the document was written. Please specify whether project or grant) 15ck18	9b. CONTRACT NO. (if appropriate, the applicable number under which the document was written)
10a. ORIGINATOR'S DOCUMENT NUMBER (the official document number by which the document is identified by the originating activity. This number must be unique to this document.) DRDC Ottawa TM 2006-227	10b. OTHER DOCUMENT NOS. (Any other numbers which may be assigned this document either by the originator or by the sponsor)

11. DOCUMENT AVAILABILITY (any limitations on further dissemination of the document, other than those imposed by security classification)

(X) Unlimited distribution
(   ) Distribution limited to defence departments and defence contractors; further distribution only as approved
(   ) Distribution limited to defence departments and Canadian defence contractors; further distribution only as approved
(   ) Distribution limited to government departments and agencies; further distribution only as approved
(   ) Distribution limited to defence departments; further distribution only as approved
(   ) Other (please specify):

12. DOCUMENT ANNOUNCEMENT (any limitation to the bibliographic announcement of this document. This will normally correspond to the Document Availability (11). However, where further distribution (beyond the audience specified in 11) is possible, a wider announcement audience may be selected.)

Unlimited

13. ABSTRACT (a brief and factual summary of the document. It may also appear elsewhere in the body of the document itself. It is highly desirable that the abstract of classified documents be unclassified. Each paragraph of the abstract shall begin with an indication of the security classification of the information in the paragraph (unless the document itself is unclassified) represented as (S), (C), or (U). It is not necessary to include here abstracts in both official languages unless the text is bilingual).

This document reports on the study of a five-element array prototype developed for communications in K-band and suitable for LTCC technology. The radiating element is an open waveguides realised in laminated technology. A novel coaxial-to-waveguide transition has also been designed as feed port for measuring the prototypes. The design, analysis, fabrication process and measurement of this antenna element were described in a previous report. To summarize, the element exhibits a 1 GHz bandwidth around a 20.7 GHz centre frequency. The element radiation pattern indicates a gain of 2.7 dBi. This new antenna is suitable for brick architecture array configuration. In an array configuration the input impedance of each radiating element is slightly perturbed by the proximity of the other antennas. The mutual coupling between the elements, however, remains below –20 dB across the bandwidth. The simulated boresight radiation pattern of a five-element array is stable over the bandwidth and the gain reaches 9.2 dBi at 20.7 GHz. These results are confirmed by the measurement. The scanned radiation patterns obtained by simulation show a good behaviour of this array for scan angles up to 50 degrees. The measured radiation patterns for several scan angles demonstrate the scanning capability of this array.

14. KEYWORDS, DESCRIPTORS or IDENTIFIERS (technically meaningful terms or short phrases that characterize a document and could be helpful in cataloguing the document. They should be selected so that no security classification is required. Identifiers such as equipment model designation, trade name, military project code name, geographic location may also be included. If possible keywords should be selected from a published thesaurus. e.g. Thesaurus of Engineering and Scientific Terms (TEST) and that thesaurus-identified. If it is not possible to select indexing terms which are Unclassified, the classification of each should be indicated as with the title.)

Antenna
Array
Phased array
laminated waveguide
LTCC Technology
Radiation pattern
Scan radiation pattern
Antenna measurement

Defence R&D Canada

Canada's leader in Defence
and National Security
Science and Technology

R & D pour la défense Canada

Chef de file au Canada en matière
de science et de technologie pour
la défense et la sécurité nationale

DEFENCE DÉFENSE

www.drdc-rddc.gc.ca